Lead Article

Acta Cryst. (1991). A47, 640-654

Oxygen Stoichiometry in High-T_c Superconductors*

BY M. MAREZIO

AT&T Bell Laboratories, Murray Hill, NJ 07974, *USA, and Laboratoire de Cristallographie-CNRS,* 38042 *Grenoble, France*

(*Received* 24 *January* 1991; *accepted* 12 *June* 1991)

Abstract

The oxygen content is one of the most important crystal chemical parameters governing the physical properties of high-T_c superconducting compounds. Studies of the oxidation process of $YBa_2Cu_3O_{6+x}$ and $Pb_2Sr_2Y_{1-x}Ca_xO_{8+\delta}$ reveal that oxygen uptake does not necessarily lead to better superconducting properties. In the former series oxygen incorporation results in a higher concentration of positive charges which are transferred from the square Cu chains to the pyramidal Cu layers. During the oxidation the most significant change consists in the movement of the apical oxygen bridging the chains to the pyramids towards the latter. The interatomic distances and, more specifically, the calculated cation valencies show that the 90 and 60 K plateaus in the T_c *vs* x curve are associated with the plateaus observed in the valency *vs* x curve for the Cu pyramidal layers. $Pb_2Sr_2YCu_3O_8$ does not become superconducting. The oxygen-depleted Cu layer inserted between two PbO layers can easily incorporate extra O atoms just like the Cu layer inserted between two BaO layers in $YBa_2Cu_3O_6$. The additional positive charges are localized on the Pb sublattice and an order between Pb^{2+} and Pb^{4+} is established. This localization hinders the charge transfer to the conducting pyramidal Cu layers and no trace of superconductivity has been detected in any oxidized sample. $Pb_2Sr_2YCu_3O_8$ becomes superconducting at ~80 K when some of the trivalent Y cations are replaced by divalent Ca. In this case the extra positive charges are transferred from the (Y, Ca) layers to the conducting pyramidal Cu layers and the compound becomes superconducting. The Cu^+ and Pb^{2+} cations remain in the reduced state because their oxidation can occur only if accompanied by a coordination increase. When heat treated at 770 K in O_2, $Pb_2Sr_2Y_{0.5}Ca_{0.5}Cu_3O_8$ behaves similarly to the undoped compound. The oxygen uptake suppresses the superconducting transition which is re-established by heat-treating the sample at the same temperature in N_2. In this case, the extra O atoms allow the Cu^+ and Pb^{2+} cations to change coordination and the extra positive charges are trapped in the (PbO)(Cu)(PbO) blocks. Moreover, the oxidation of the Cu^+ and Pb^{2+} cations induces the displacement of the apical oxygen of the pyramidal layers. A charge transfer towards the (PbO)(Cu)(PbO) blocks takes place and consequently the superconducting state is suppressed.

Introduction

The oxygen stoichiometry in high-T_c superconductors is a crucial physical-chemical problem because all these compounds are oxides and, moreover, because the superconducting properties are closely related to the mixed-valency states contained in these compounds, mixed-valency states which are controlled by the oxygen stoichiometry.

Table 1 shows a non-exhaustive list of high-T_c oxide superconductors. At the top of the list one sees $YBa_2Cu_3O_{6+x}$ (Wu *et al.*, 1987), for which the value of x is one of the most important parameters for the occurrence of superconductivity. At the bottom one sees the only non-copper high-T_c superconductor (Cava, Batlogg, Krajewski, Farrow *et al.*, 1988; Mattheiss, Gyorgy & Johnson, 1988) for which the oxygen stoichiometry is just as important as for the Cu-based superconductors. The mixed valency for Bi is due to the K doping, but the oxygen stoichiometry is a crucial parameter because small departures from O_3 produce structures different from the simple perovskite, the only phase which becomes superconducting. (Hinks *et al.*, 1988; Schneemeyer *et al.*, 1988).

Just above $(K,Ba)BiO_3$ are the latest reported superconductors, $La_{1.6}Sr_{0.4}CaCu_2O_6$. This is the second member of the homologous series $La_2Ca_{n-1}Cu_{2+2n}$ of which La_2CuO_4 is the first member. Many authors have prepared this compound and found it non-superconducting. Only recently has it been prepared with the correct stoichiometry and found to become superconducting at 60 K (Cava, Batlogg *et al.*, 1990).

In this article I shall not discuss the oxygen-stoichiometry problem for every high-T_c superconductor as such discussion would be monumental. I

* *Editorial Note*: This invited paper is one of a series of comprehensive Lead Articles which the Editors invite from time to time on subjects considered to be timely for such treatment.

0108-7673/91/060640-15$03.00

Table 1. *Some high-T_c oxide superconductors*

$YBa_2Cu_3O_{6+x}$	
$Pb_2Sr_2Y_{1-x}Ca_xCu_3O_{8+\delta}$	
$La_{1.85}Sr_{0.15}CuO_4$	T phase
$La_2CuO_{4+\delta}$	T phase
$(Nd, Ce)_2CuO_4$	T' phase
$(La, Tb)_2CuO_4$	T^* phase
$Bi_2Sr_2Ca_{n-1}Cu_nO_{2n+4}$	
$Tl_mBa_2Ca_{n-1}Cu_nO_{2n+m+2}$	
$La_{1.6}Sr_{0.4}CaCu_2O_6$	
$(K, Ba)BiO_3$	

shall limit myself to the cases of the $YBa_2Cu_3O_{6+x}$ and the $Pb_2Sr_2Y_{1-x}Ca_xCu_3O_{8+\delta}$ series (Cava, Batlogg, Krajewski, Rupp *et al.*, 1988). I would also like to point out that this article is not intended to be a review of all the work done on these two series. My purpose is to show the importance of the oxygen stoichiometry and I have chosen these two series because the oxygen incorporation produces opposite effects on their physical properties. In the former series an increase of x above $\sim 0{\cdot}4$ induces the superconducting state at ~ 60 K, whereas in the latter series an increase of δ up to $\sim 1{\cdot}8$, for the compound with $x = 0$, does not induce any superconductivity and for the compound with $x = 0{\cdot}5$, which is superconducting, an incorporation of oxygen above O_8 suppresses the superconducting state.

If we could understand these opposite behaviors from the structural point of view, at least for these two series, we would be able to determine what role the oxygen stoichiometry plays in relation to the superconducting properties and this could guide us to understand similar problems in other systems.

$YBa_2Cu_3O_{6+x}$

To illustrate the effect of the oxygen stoichiometry on the superconducting properties of $YBa_2Cu_3O_{6+x}$ I will concern myself with the data published by Cava, Hewat *et al.* (1990). These authors prepared ten samples with different values of x (0·95, 0·84, 0·81, 0·78, 0·73, 0·64, 0·58, 0·45, 0·35 and 0·00) by the Zr-gettered technique, which allows one to prepare very homogeneous samples. The average structure was determined by powder neutron diffraction while the oxygen ordering was checked by electron diffraction and the T_c's were measured by magnetization measurements. Similar studies have also been published by a number of authors, the most recent ones being those carried out by Jorgensen *et al.* (1990). The samples used by the latter authors were prepared by a different technique and their results differ in some details from those of Cava, Hewat *et al.* (1990). It would be very interesting to discuss these differences, but this is outside the purpose of my thesis.

Fig. 1(*a*) shows the structure of $YBa_2Cu_3O_6$ which is tetragonal (Bordet, Chaillout, Capponi, Chenavas & Marezio, 1987; Santoro *et al.*, 1987) and can be described as an oxygen-deficient perovskite structure. The large cations, yttrium and barium, form layers perpendicular to the c axis. Because these layers are ordered with the sequence YBaBaYBaBa, the c axis is tripled. The oxygen vacancies are ordered as well, so that the coordination of barium and yttrium decreases from twelve to eight, whereas the coordination of the smaller Cu cations decreases from six (octahedral) to two (stick) for Cu1 and to five (pyramidal) for Cu2. The Cu1 atoms or the O–Cu1–O sticks form infinite chains along the crystallographic axes of the perovskite cell. The $Cu2O_5$ pyramids form layers *via* corner sharing with two of these layers sandwiching an oxygen-depleted yttrium layer. There are two types of O atoms, O1 linking the sticks to the pyramids (the apical oxygen) and O2 forming the base of the pyramids. $YBa_2Cu_3O_6$ has tetragonal symmetry and is an antiferromagnetic semiconductor (Tranquada *et al.*, 1987). One of the most important physical-chemical properties of this compound is its ability to incorporate oxygen up to one atom per $YBa_2Cu_3O_6$ molecule (Strobel, Capponi, Chaillout, Marezio & Tholence, 1987). These extra O atoms (O4) are located along one of the perovskite axes to form, together with the O–Cu–O sticks, infinite chains of corner-sharing squares. The incorporation of oxygen does not take place at random but, as shown by electron microscopy, it occurs by rows (Beyers *et al.*, 1989) and the Cu1 cations of any given oxidized row increase their valency from 1+ to 3+. Such a mechanism of incorporation avoids the formation of unstable three-coordinated Cu cations. The oxidized rows order in the structure to form superstructures. One of these is shown in Fig. 1(*b*) which corresponds to the compound with $x = 0{\cdot}5$. In this structure every other stick chain along the a axis has become a square chain, resulting in the doubling of the a axis. The orthorhombic structure ($a = 2_{ap}$, $b \simeq {}_{ap}$) contains three types of Cu cations, having pyramidal, square and stick coordinations, respectively (Alario-Franco, Chaillout, Capponi, Chenavas & Marezio, 1987).

When all the O4 positions have been filled one obtains the structure of superconducting $YBa_2Cu_3O_7$ shown in Fig. 1(*c*). This structure is orthorhombic with $a \simeq a_p$, $b \simeq a_p$ and $c = 3a_p$ (Siegrist, Sunshine, Murphy, Cava & Zahurak, 1987; Beno *et al.*, 1987; Greedan, O'Reilley & Stager, 1987; Capponi *et al.*, 1987; Beech, Miraglia, Santoro & Roth, 1987; David *et al.*, 1987; Izumi *et al.*, 1987; François, Walker, Jorda, Yvon & Fischer, 1987; Cox, Moodenbaugh, Hurst & Jones, 1987). All stick-coordinated Cu1 cations have become squarely coordinated. The Ba cations have increased their coordination from eight to ten while the Y cations are still surrounded by eight O atoms. There are four crystallographically independent O atoms. Because of the orthorhombic symmetry, O2 and O3 forming the base of the pyramids surrounding Cu2 have become

crystallographically independent. O4 is the mobile oxygen forming, with the apical oxygen O1, the squares around Cu1. The two corner-sharing pyramidal layers sandwiching the oxygen-depleted yttrium layer constitute the structural feature which seems to be essential for superconductivity in copper-based high-T_c superconductors.

Fig. 2 shows DC (direct current) magnetization as a function of temperature for some of the samples, measured on cooling in a field of 39·8 A m^{-1}. Fig. 3 shows the superconducting transition temperatures T_c for the ten samples of $YBa_2Cu_3O_{6+x}$. The two-plateau feature at approximately 90 and 60 K and a broad intermediate T_c region can be seen. This feature

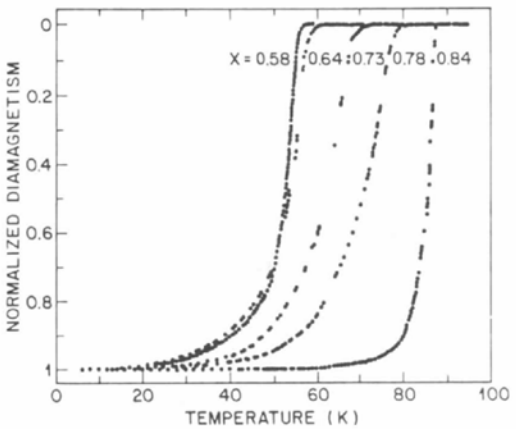

Fig. 2. Superconducting transitions for samples between the 90 and 60 K plateaus.

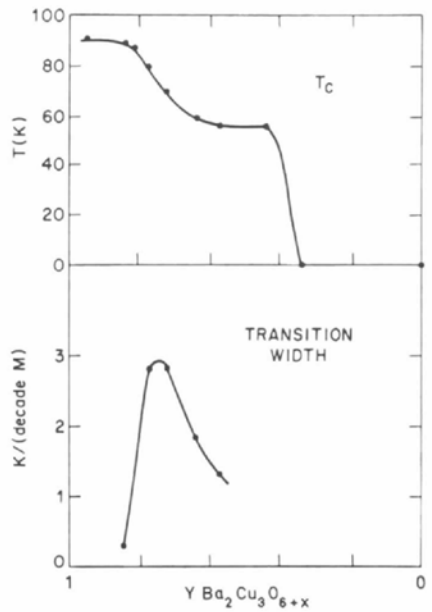

Fig. 3. Superconducting transition temperature T_c as a function of x (top) and the width of the superconducting transitions in kelvins per decade of magnetization (bottom).

was first reported by Cava (1987). Superconductivity abruptly disappears for $x < 0{\cdot}45$. T_c has been determined from the onset of diamagnetism on a linear scale. The bottom of Fig. 3 shows the width of the transitions in kelvins per decade of magnetization. The superconducting transitions are sharpest in the regions of the plateaus. A simple interpretation of this feature would be that only two well defined phases exist, one with $T_c \simeq 90$ K and one with $T_c \simeq 60$ K, the phases in between would be mixtures of these two end phases. Unfortunately, such a simplistic model is not corroborated by electron microscopy data (Beyers *et al.*, 1989) and the real situation is much more complicated than the two-phase system. It has been proposed (Cava, Hewat *et al.*, 1990) that each different short-range ordering of the O atoms has its own characteristic T_c between 90 and 60 K and that their similarity in composition makes their isolation in pure form difficult.

Fig. 4 shows the electron diffraction pattern perpendicular to the [001] axis for the sample with $x = 0{\cdot}58$. It can be seen that the crystallite is twinned by the (110) plane and consequently both a and b axes are doubled instead of the a axis only. It should be noted that the superstructure spots are somewhat elongated along the [100] direction. This is an indication that the sequence of full (square) and empty (stick) chains has a short correlation length. In this sample, which corresponds to $x = 0{\cdot}58$, there must be more full than empty chains. Adjacent full–full chains must occur shortening the correlation length. Table 2 gives the type of superstructure observed in the basal plane for each sample along with the superconducting transition temperature.

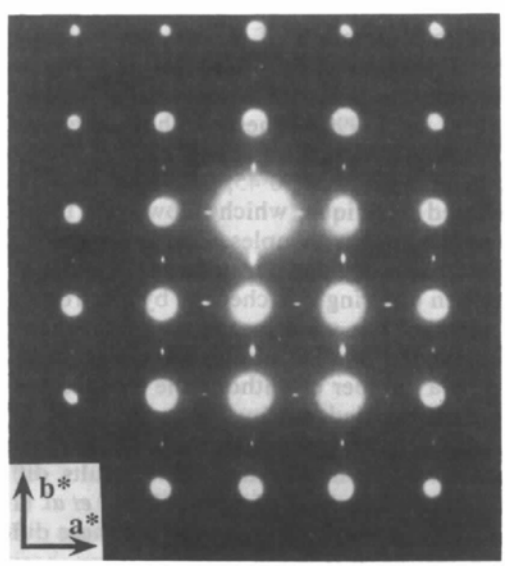

Fig. 4. Electron diffraction pattern perpendicular to [001] from orthorhombic $YBa_2Cu_3O_{6\cdot58}$ showing typical twinning with a long-range superstructure in the *ab* plane.

Table 2. *Superconducting transition temperatures (T_c) and superstructures observed by electron diffraction for $YBa_2Cu_3O_{6+x}$ samples prepared at 710 K (from Cava, Hewat et al., 1990)*

x	T_c (K)	Superstructure
0·95	90	None
0·84	88	None
0·81	86	Diffuse lines
0·78	79	Diffuse lines
0·73	69	Diffuse lines $+3a$ spots
0·64	59	Elongated $2a$, some diffuse $3a$ spots, some $\frac{1}{4}, \frac{1}{4}, 0$ spots
0·58	56	Sharp $2a$ spots
0·45	56	Sharp $2a$ spots
0·35	—	None
0·00	—	None

Fig. 5 shows the electron diffraction pattern perpendicular to the [010] axis for the same sample with $x = 0{\cdot}58$, where the doubling of the a axis is also seen. It is interesting to note that the superstructure spots are well defined along the three directions which indicates that the samples, at least in the range $0{\cdot}6 > x > 0{\cdot}4$, are well ordered as far as the oxygen distribution is concerned. The same photograph taken with samples prepared with techniques different from the Zr-gettered one showed somewhat continuous lines at $(h+\frac{1}{2}, 0, l)$ indicating decorrelation along the c axis of the order occurring in the basal plane.

Fig. 6 shows the lattice parameters of $YBa_2Cu_3O_{6+x}$ as a function of x. One can see the abrupt drop of the c parameter between $x = 0{\cdot}35$ and $x = 0{\cdot}45$. It is between these two compositions that the symmetry of the powder pattern changes from tetragonal ($a = b$) to orthorhombic ($a \neq b$). The only true tetragonal structure is that of $YBa_2Cu_3O_6$ where all the O4 sites are empty. As soon as the first O atoms are incorporated in the structure along the Cu1 rows, a local orthorhombic distortion occurs. At the given oxygen concentration the local distortions become cooperative and the crystal symmetry changes to orthorhombic. Fig. 7 shows the variation of the cell volume and of the orthorhombicity defined as $200(a-b)/(a+b)$, as a function of x. The tetragonal-to-orthorhombic transition is visible in both curves.

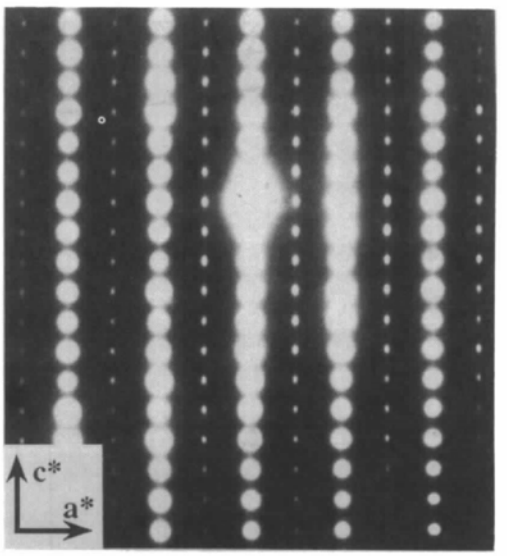

Fig. 5. Electron diffraction pattern perpendicular to [010] from orthorhombic $YBa_2Cu_3O_{6\cdot58}$ showing long-range order also along the c axis.

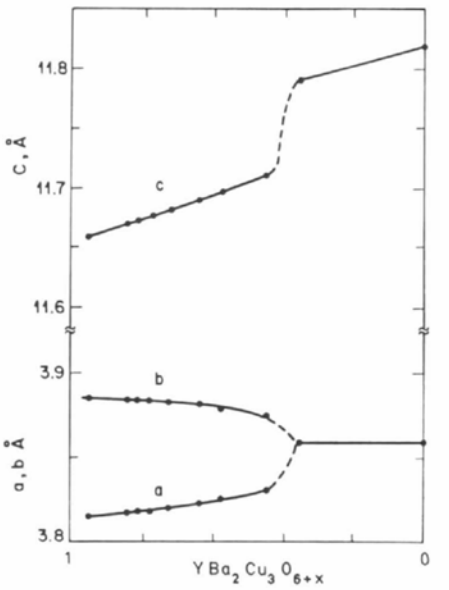

Fig. 6. Cell parameters for $YBa_2Cu_3O_{6+x}$.

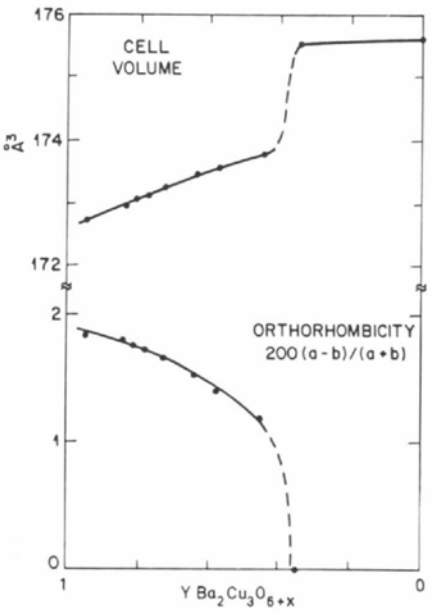

Fig. 7. Cell volume and orthorhombicity for $YBa_2Cu_3O_{6+x}$.

Figs. 8–11 show the variations of the individual cation–oxygen distances as a function of x. The Cu1–O1 distance, that is the distance between the stick-coordinated Cu to the apical oxygen, remains constant in the tetragonal region and increases with increasing x in the orthorhombic region. It should be noted that in the tetragonal region the Cu1–O1 distance is insensitive to the incorporation of O atoms although these atoms are linked to Cu1. In the orthorhombic region the Cu1–O1 distance, which is along the c axis, increases despite the decrease of the c axis. The Cu1–O4 distance, which is measurable only for the orthorhombic or nearly so samples increases slightly from $x = 0{\cdot}45$ to $x = 0{\cdot}58$ and then remains constant up to $x = 1$.

The variation as a function of x of the Cu2–O1 distance, that is that between the pyramidal coordinated Cu2 cation to the apical oxygen O1, is quite

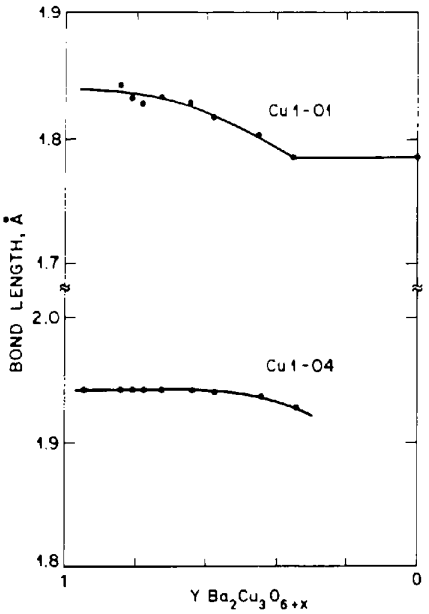

Fig. 8. Chain copper (Cu1) to apical oxygen (O1) bond lengths (top) and chain copper to mobile oxygen (O4) bond lengths (bottom) for $YBa_2Cu_3O_{6+x}$.

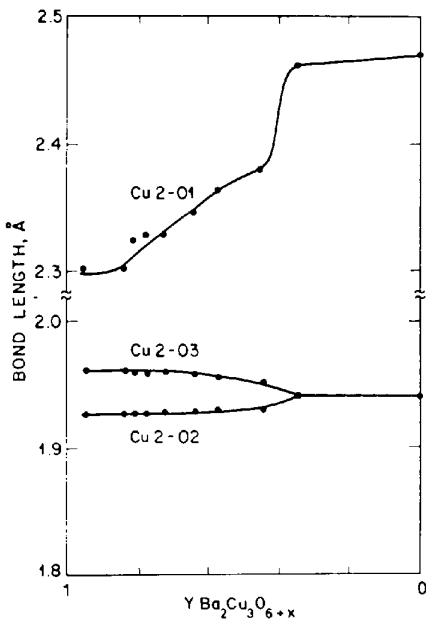

Fig. 9. Planar copper (Cu2) to apical oxygen (O1) and to basal oxygens (O2 and O3) bond lengths for $YBa_2Cu_3O_{6+x}$.

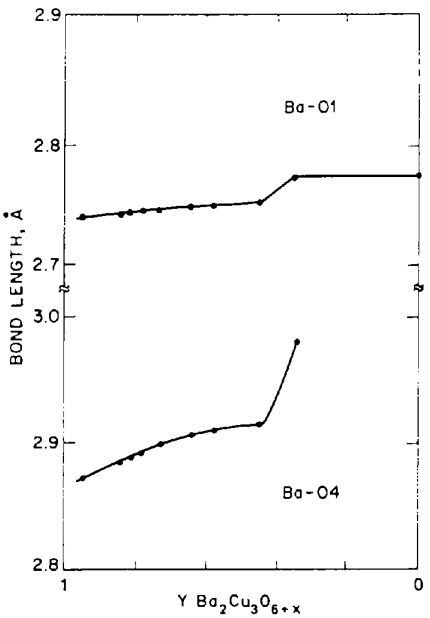

Fig. 10. Ba–O1 and Ba–O4 bond lengths for $YBa_2Cu_3O_{6+x}$.

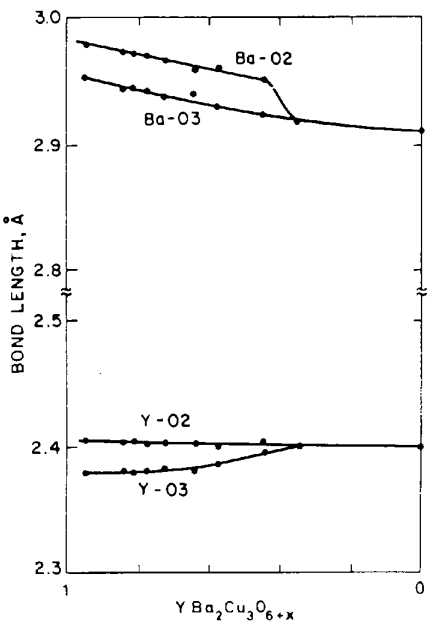

Fig. 11. Bond lengths of Ba and Y to O2 and O3 for $YBa_2Cu_3O_{6+x}$.

interesting. It decreases slightly in the tetragonal region on going from $x = 0$ to $x = 0{\cdot}35$. The decrease becomes abrupt between $x = 0{\cdot}35$ and $x = 0{\cdot}45$. The abrupt drop of the c axis at this transition is surely related to the decrease of the Cu2-O1 distance. In the orthorhombic region this distance decreases rapidly between $x = 0{\cdot}45$ and $x = 0{\cdot}84$ and then remains constant between $x = 0{\cdot}84$ and $x = 1$. This last plateau corresponds to the 90 K superconductivity. The Cu2-O2 and Cu2-O3 distances show a normal variation. Since O2 and O3 are equivalent in the tetragonal phase only one value is shown, which does not vary with increasing x. At the transition O2 and O3 become inequivalent and the two distances differ by about 1%.

The variation of the Ba-O distances shows that the incorporation of oxygen induces the Ba cations to move away from the Cu2-O2-O3 plane toward the O1 plane. Consequently, Ba-O2 and Ba-O3 increase for increasing x whereas Ba-O1 decreases with a step-like behavior at the transition. Since the Ba cations move towards O1 and therefore towards O4, the distance Ba-O4 decreases with increasing x. The Y atoms are not affected by the incorporation of oxygen as the Y-O distances have a normal behavior as a function of x. The Y-O distance of the tetragonal phase splits into two distances, Y-O2 and Y-O3, at the tetragonal-to-orthorhombic transition because of the inequivalence in the orthorhombic structure between O2 and O3.

In ionic structures one can calculate the cation and anion effective valencies from the interatomic distances. Based on the ideas of Pauling, Zachariasen and Brown, there are several formulations from which the bond strengths can be derived from the corresponding bond lengths. The sum of the bond strengths around a given atom (cation or anion) gives its effective valency. Here we have employed the formula and the constants derived by Brown & Altermatt (1985). The values obtained for Cu1, Cu2, Ba and Y are plotted in Figs. 12 and 13.

If one assumes that the formal valency of the O atoms in $YBa_2Cu_3O_6$ is 2−, that of the Y, Ba, Cu1 and Cu2 cations is 3+, 2+, 1+ and 2+, respectively. One can assign integer values to the two types of Cu cations because the stick coordination is only appropriate for the Cu^+ cations. The calculated valencies by the bond-strength-bond-length relationship are 1·3 and 2·13 for Cu1 and Cu2, respectively. These values differ substantially from those quoted above and might indicate, in view of the fact that the bond-strength-bond-length relationship only applies to structures with strong ionic character, that the Cu–O bonds must be at least partially covalent. On the other hand, deviations of the bond-strength sum from the expected valency of a cation are also considered to reflect internal stresses on the cation coordination polyhedra, due to constraints imposed by the remainder of the structure (Brown, 1989). Thus, the absolute calculated values of the effective valencies may not be precise, but the changes are meaningful quantities.

The average valency of the Cu1 cations (chain Cu) increases linearly from 1·3 for $x = 0$ to 2·4 for $x = 1$, independently of the symmetry of the phase and whether the material is semiconducting or superconducting. This type of variation is justified because the incorporated O atoms are bonded directly to Cu1 and the positive charges which are created contribute to increase the valency of this cation. On the contrary, the valency of the Cu2 cations (planar Cu) displays a remarkable non-linear variation with oxygen stoichiometry. Although positive charges are created in the structure, the planar Cu valency does not vary in the tetragonal phase. Between $x = 0{\cdot}35$ and $x = 0{\cdot}45$, that is at the appearance of superconductivity, the planar Cu valency exhibits an abrupt increase of 0·05 v.u./Cu. There is a plateau near $x = 0{\cdot}5$ followed by a gradual increase of 0·03 v.u./Cu from $x = 0{\cdot}6$ to $x = 0{\cdot}8$. Between $x = 0{\cdot}8$ and $x = 1$ the valency of the planar Cu is constant.

The behavior of the planar Cu valency as a function of x indicates that, as oxygen is incorporated between $x = 0$ and $x = 0{\cdot}35$, all the generated positive charges remain on the chain Cu cations. When about one third of these cations have become squarely coordinated, a charge transfer occurs from the chain to the planar Cu cations and superconductivity appears. At this point, the charge transfer seems to stop and the valency of the planar Cu cations remains approximately constant between $x = 0{\cdot}45$ and $x = 0{\cdot}64$. When

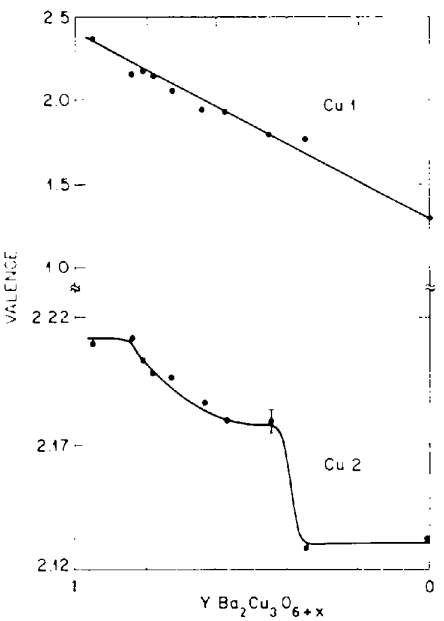

Fig. 12. Calculated valencies for the chain Cu1 and planar Cu2 cations as a function of oxygen stoichiometry in $YBa_2Cu_3O_{6+x}$.

two thirds of the chain Cu cations have become squarely coordinated, a more gradual increase of the planar Cu valency occurs up to $x = 0{\cdot}84$ Then the charge transfer stops again and a second plateau is established.

Fig. 13 shows the variations of the calculated valencies for the Ba and Y cations which would be expected, given the ionicity of their bonds to oxygen, to be 2+ and 3+, respectively. As can be seen, both valencies vary as a function of x. The variation of the Ba valency from 1·8 to 2·2 can be interpreted as a change in geometric stress induced by the rest of the structure. The only unstressed structure, as far as the Ba cations are concerned, is that of $YBa_2Cu_3O_{6\cdot5}$, whereas the Ba coordination polyhedron is too large for $YBa_2Cu_3O_6$ and too small for $YBa_2Cu_3O_7$. A model for calculating cation valencies from a bond-strength sum which takes into account the geometrical stresses has recently been proposed (Brown, 1990).

The calculated Y valency is about 2·85 for the tetragonal or nearly tetragonal samples. It increases to about 2·9 for the orthorhombic ones. These values, lower than the expected 3+, are also due to geometrical stresses and to the covalency of the Y–O bonds. The step-like variation at about $x = 0{\cdot}5$ is due to a change in these geometrical stresses. This is suggested by the variation with x of the individual bond lengths, Y–O2 and Y–O3. The former distance is nearly constant over the whole stoichiometry range while the latter increases to meet the Y–O2 bond length at the orthorhombic-to-tetragonal transition.

The variation of the valency of the planar Cu cations, Cu2, as a function of x and that of the superconducting transition temperatures for $YBa_2Cu_3O_{6+x}$ are shown next to each other in Fig. 14. The correlation is striking: the valency shows two-plateau behavior as does T_c. Thus, the change from 90 to 60 K superconductors is associated with a gradual decrease of positive charge for the planar Cu cations of approximately 0·03 v.u./Cu, which corresponds to a decrease of the 'hole' concentration. The transition from the 60 K superconductor to the tetragonal semiconductor involves an abrupt decrease of the positive charge for the planar Cu cations of approximately 0·05 v.u./Cu. This is the first time that this correlation has been so clearly made.

$Pb_2Sr_2Y_{1-x}Ca_xCu_3O_{8+\delta}$

The second series I discuss is that discovered by Cava and his collaborators in 1988 whose prototype is $Pb_2Sr_2YCu_3O_8$. Later, the same series was independently reported by Subramanian *et al.* (1989). The structure of this compound, schematized in Fig. 15, contains the usual feature of all copper-based high-T_c superconductors, that is the double copper-oxygen pyramidal layers sandwiching the oxygen-depleted yttrium layer. The Sr cations together with the apical oxygen of the pyramids form (SrO) layers. The double pyramidal layers are separated by a block composed of two PbO layers sandwiching one oxygen-depleted Cu layer; this block represents the unique feature of this structure (Cava, Batlogg, Krajewski, Rupp *et al.*, 1988).

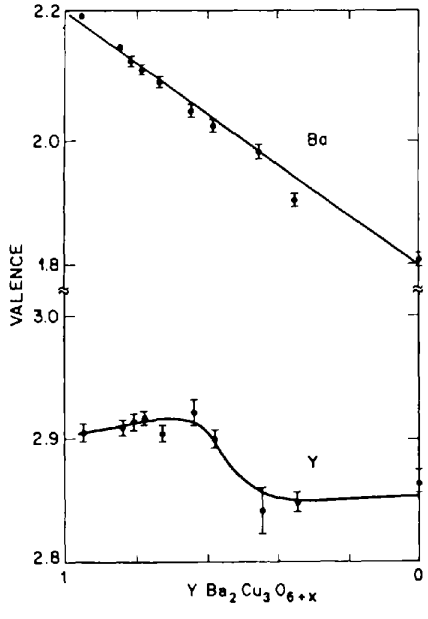

Fig. 13. Calculated valencies for the Ba and Y cations as a function of oxygen stoichiometry in $YBa_2Cu_3O_{6+x}$.

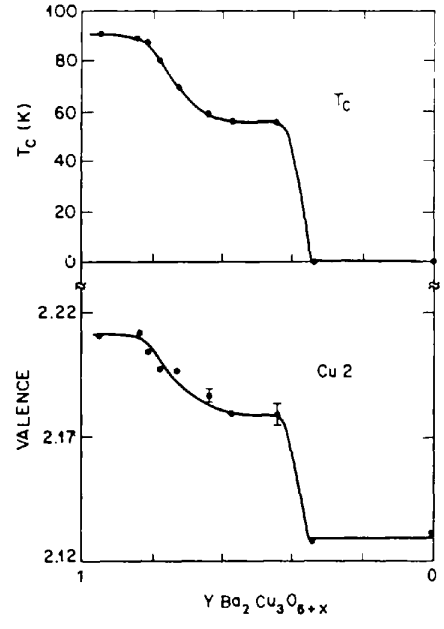

Fig. 14. Comparison of T_c and calculated valency of the planar Cu cations as a function of oxygen stoichiometry in $YBa_2Cu_3O_{6+x}$.

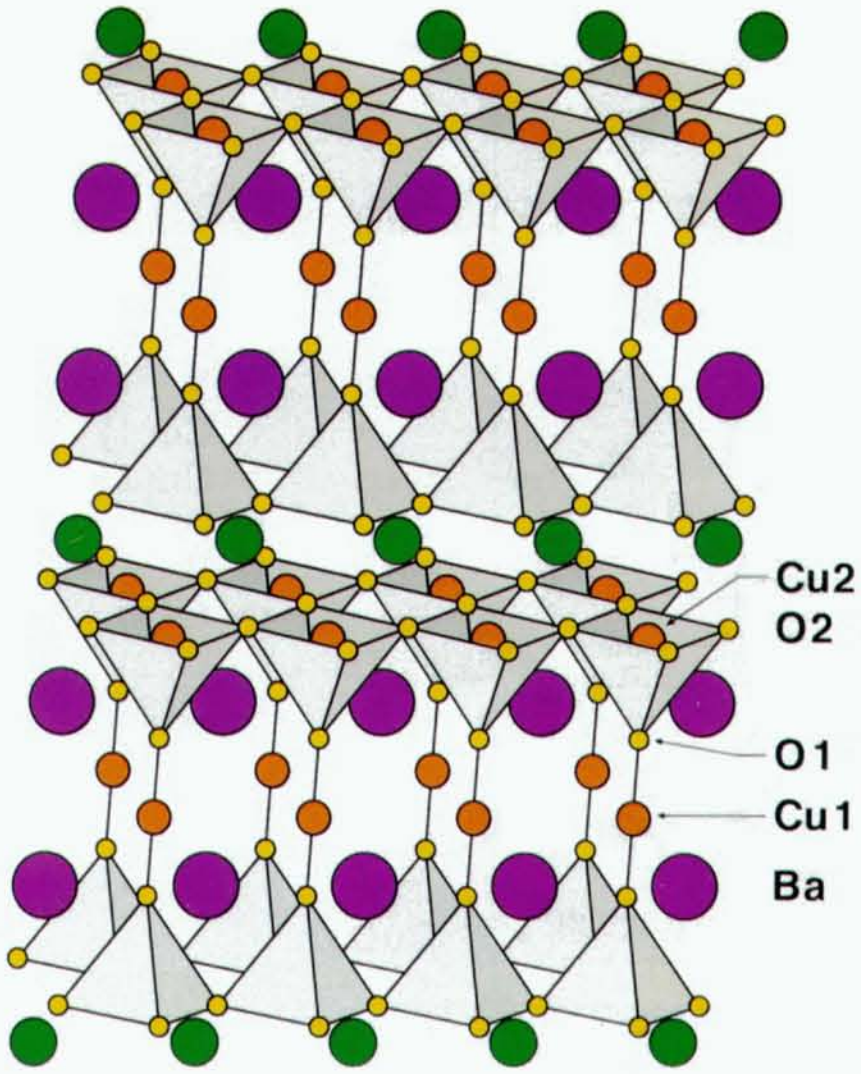

(*a*)

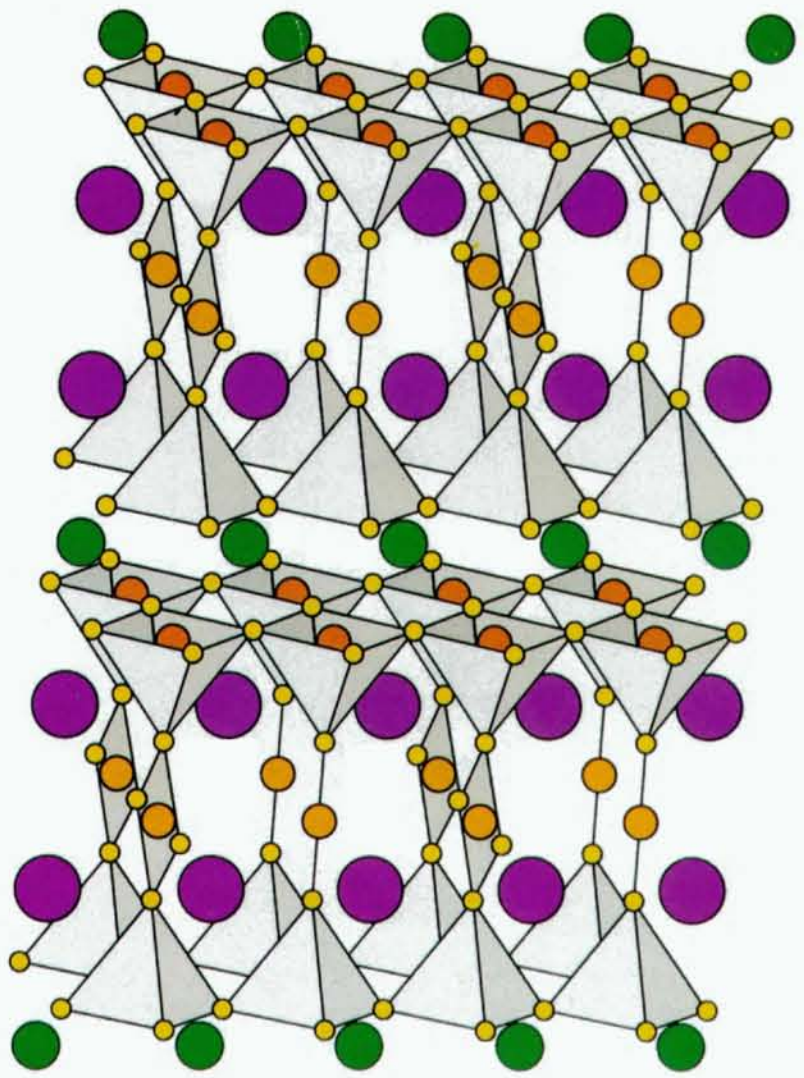

(*b*)

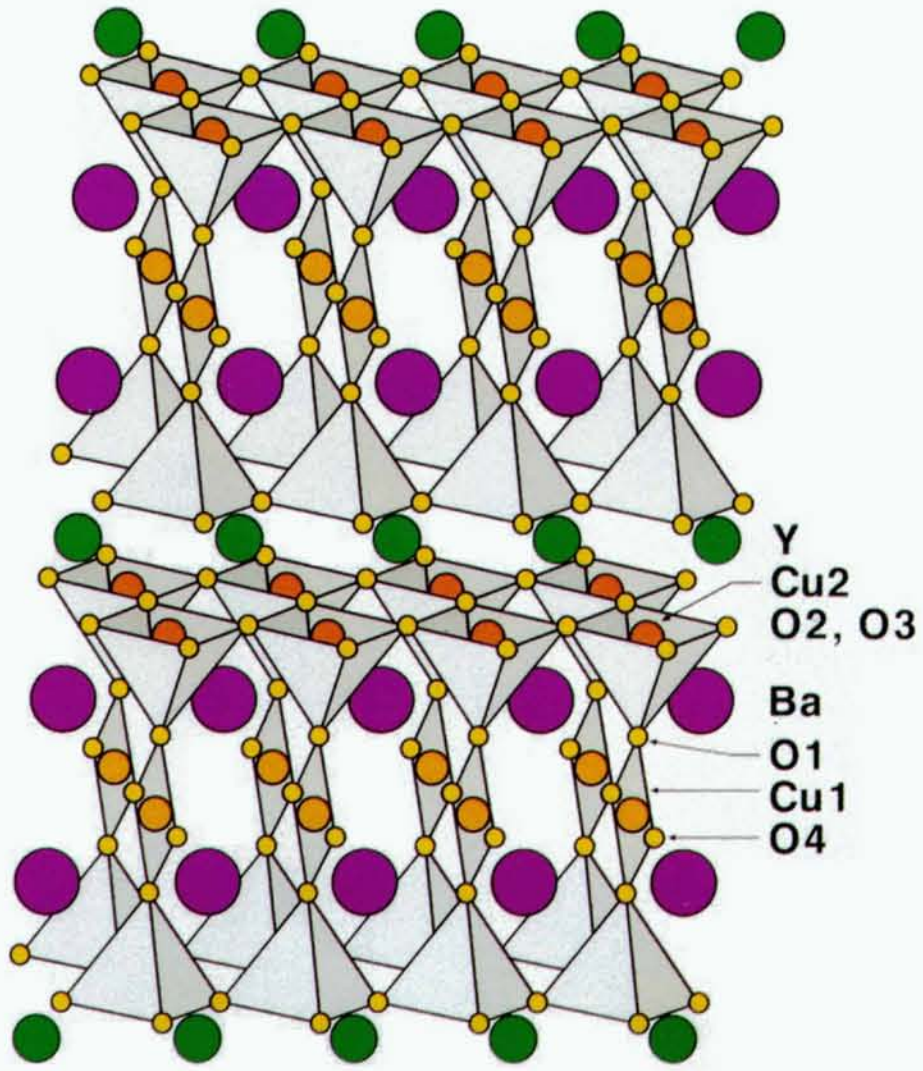

(*c*)

Fig. 1. (*a*) The structure of $YBa_2Cu_3O_6$. (*b*) The structure of $YBa_2Cu_3O_{6.5}$. (*c*) The structure of $YBa_2Cu_3O_7$.

[*to face page* 646

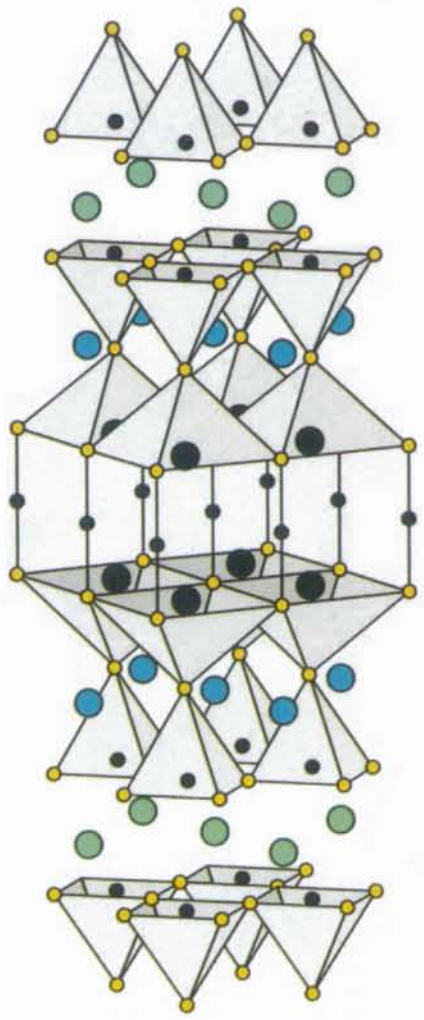

Fig. 15. Schematic representation of the crystal structure of $Pb_2Sr_2YCu_3O_8$ where the coordination polyhedra are outlined. Small black and yellow dots are copper and oxygen, respectively; black circles, lead; light blue circles, strontium; green circles, yttrium.

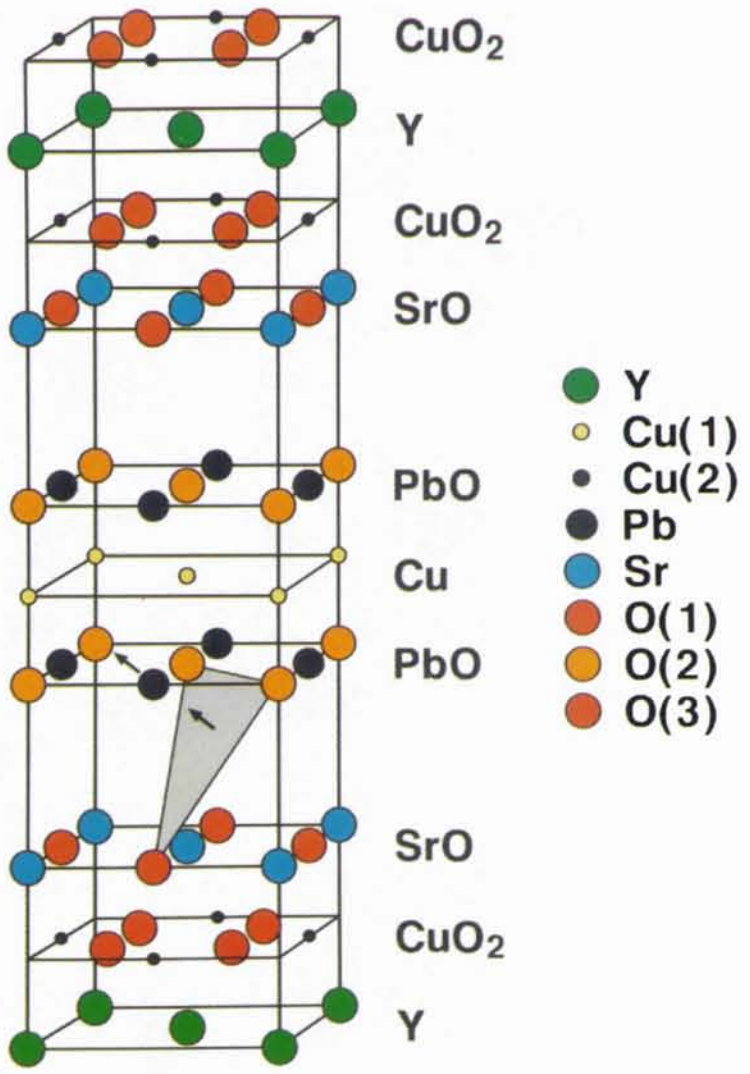

Fig. 17. Schematic representation of the structure of $Pb_2Sr_2YCu_3O_8$ viewed as a sequence of (AO) and (BO_2) layers, perpendicular to the c axis, in which the single atoms are shown. The arrow perpendicular to the triangle of O atoms indicates the direction along which these atoms are displaced. The arrow associated with the Pb cation represents the direction along which the 'lone pair' of electrons points.

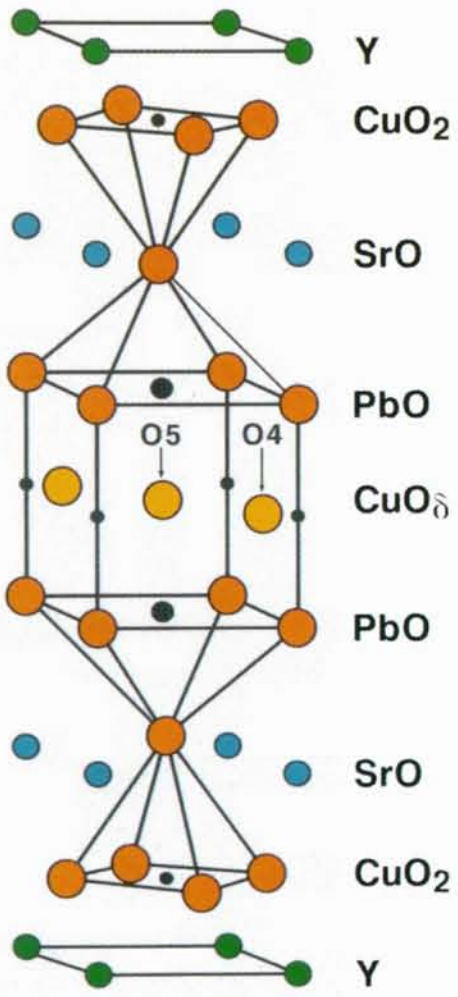

Fig. 23. A schematic representation of the $Pb_2Sr_2YCu_3O_{9.5}$ structure.

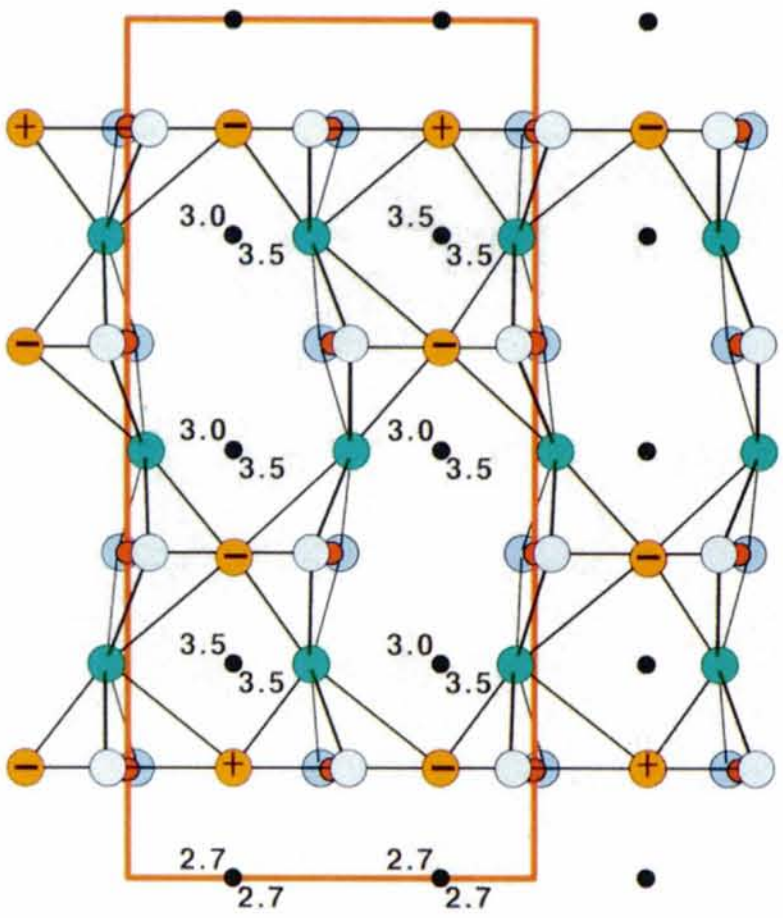

(*a*)

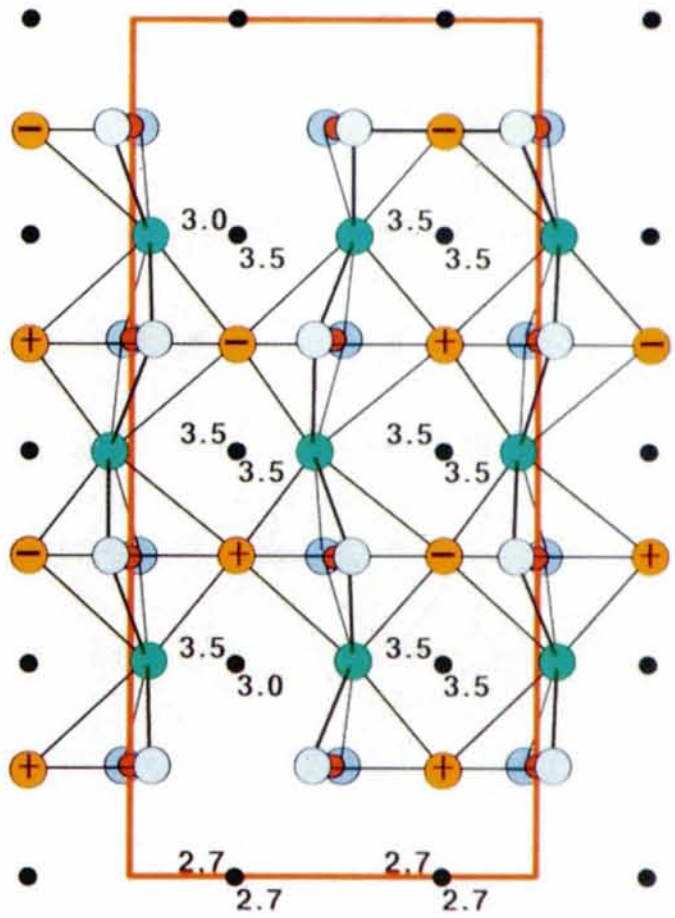

(*b*)

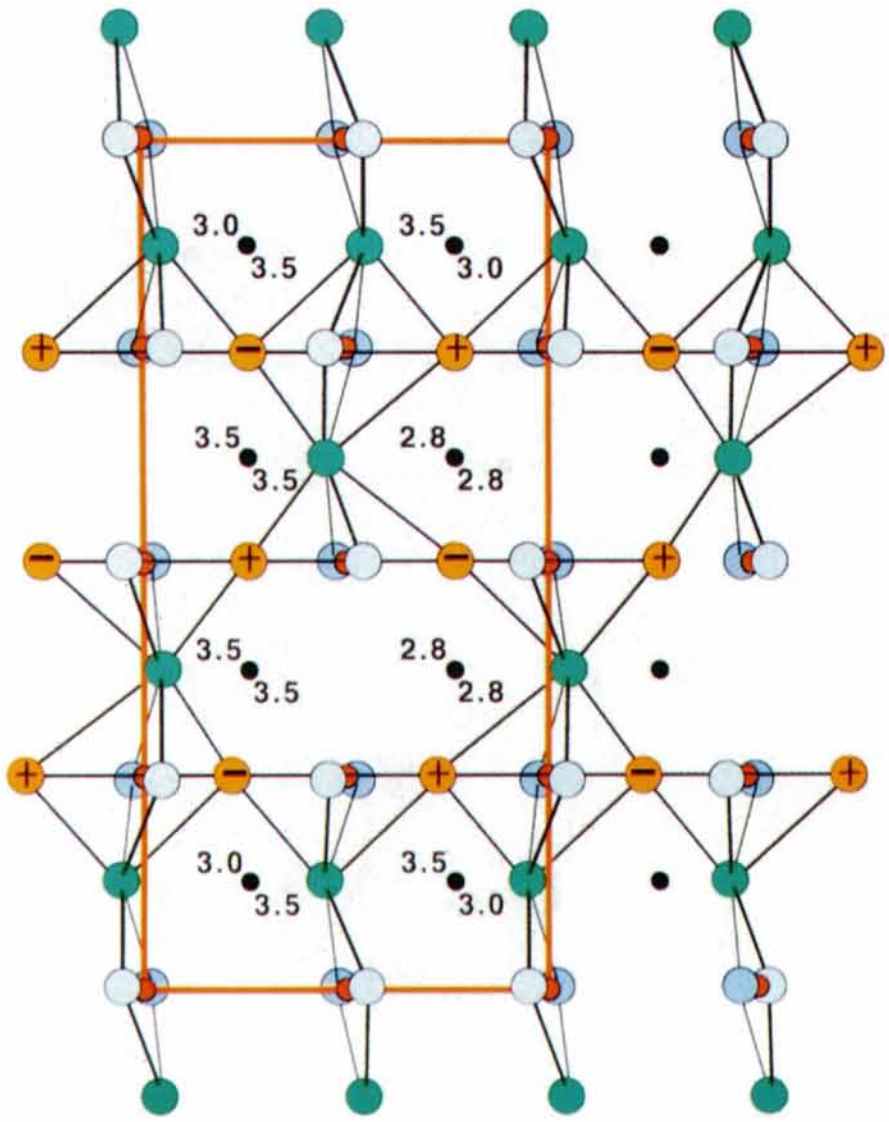

(*c*)

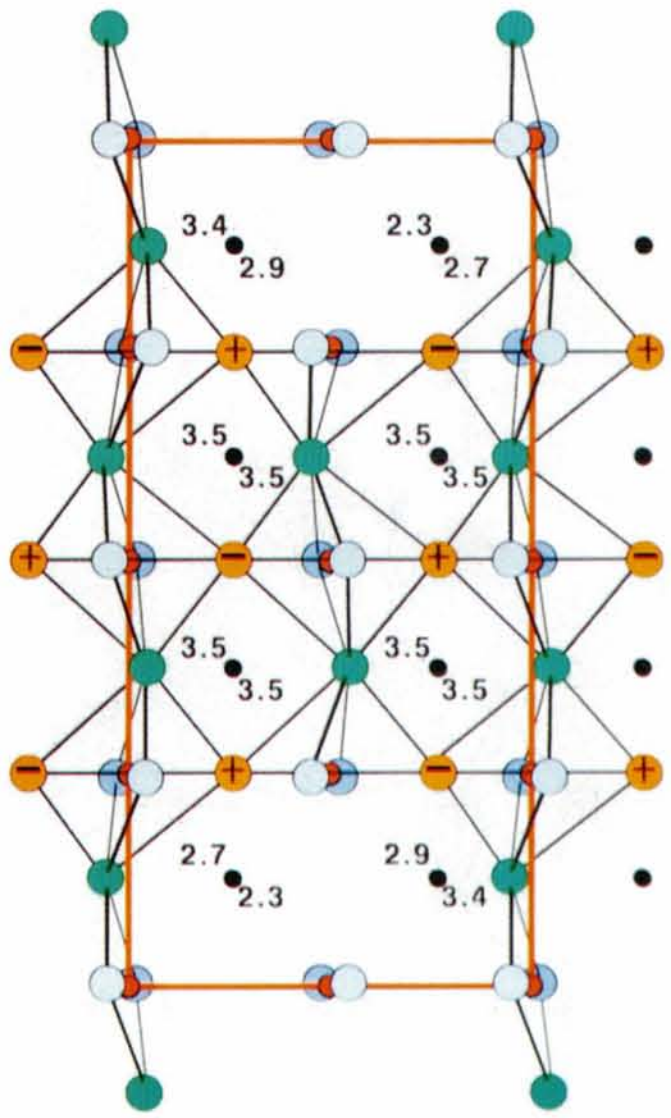

(*d*)

Fig. 25. (*a*), (*b*), (*c*), (*d*) Projections on the *ab* plane of the (PbO)($CuO_{1.5}$)(PbO) block of the $Pb_2Sr_2YCu_3O_{9.5}$ structure. The ($CuO_{1.5}$) layer comprises Cu1, O4 and O5 atoms represented by red dots, orange and green circles, respectively. The + and the − inside the orange circles indicate the displacements along the *c* axis. The (PbO) layers comprise Pb and O2 atoms, the former are represented by black dots and the latter by blue circles. The O2 atoms of the layer above and those of the layer below the ($CuO_{1.5}$) layer are light blue and blue, respectively. The $4a \times 2b$ supercells are outlined in orange. Note that the occupancy of split O atoms is ordered in all directions. Decorrelation would induce changes in the coordination and valency of the Pb and Cu atoms.

In $Pb_2Sr_2YCu_3O_8$, integer formal valencies can be assigned to all atoms, namely Pb^{2+}, Sr^{2+}, Y^{3+}, Cul^{+} (coordinated to two O atoms), $Cu2^{2+}$ (pyramidally coordinated) and O^{2-}. Because of the low formal average valency for the Cu cations (1·67+), it is not surprising that $Pb_2Sr_2YCu_3O_8$ was found to be an antiferromagnetic semiconductor (Cava, Marezio, Krajewski, Peck, Santoro & Beech, 1989) like $YBa_2Cu_3O_6$ and La_2CuO_4.

The structures of the high-T_c superconductors can be easily compared to each other by using the classification proposed by Santoro, Beech, Marezio & Cava (1988). In this classification the structures are described as built of (AO) and (BO_2) layers stacked to form either perovskite or NaCl blocks. The sequence corresponding to $Pb_2Sr_2YCu_3O_8$ is given in Fig. 16 together with those of $YBa_2Cu_3O_6$ (on the right) and $Bi_2Sr_2CaCu_2O_8$ (on the left). It can be seen that the structure of $Pb_2Sr_2YCu_3O_8$ is very similar to that of $YBa_2Cu_3O_6$. The difference between the two lies in the insertion in the former structure of (PbO) layers between the (SrO) and Cu layers. On the other hand, the difference between $Pb_2Sr_2YCu_3O_8$ and $Bi_2Sr_2CaCu_2O_8$ is even simpler because it consists of the insertion of oxygen-depleted Cu layers between two successive (PbO) layers. The total charge of a block comprising two (BiO) layers as in $Bi_2Sr_2CaCu_2O_8$ is 2+ whereas that of the block comprising two (PbO) layers would be zero. The insertion of a monovalent Cu layer brings the charge of the (PbO)(Cu)(PbO) block up to 1+. From the sequence of $Pb_2Sr_2YCu_3O_8$ it can be seen that the Pb cations are surrounded by five O atoms arranged as a square pyramid which is not the appropriate coordination for Pb^{2+} cations with the lone pair of electrons.

Fig. 17 shows another schematic representation of the structure of $Pb_2Sr_2YCu_3O_8$ viewed as a sequence of layers, but in which the various atoms are shown. This structure is orthorhombic with cell parameters $a \simeq 2^{1/2}a_p$, $b \simeq 2^{1/2}a_p$ and $c \simeq 15{\cdot}7$ Å. Its refinement based on powder neutron data was carried out in the *Cmmm* space group (Cava *et al.*, 1989). It showed that the O2 atoms of the PbO layers have large thermal parameters along the a and b axes. This was interpreted as due to a static disorder. Accordingly, in the subsequent refinements, the O2 atom at (00z) of the *Cmmm* space group was split over the four general positions (xyz) as shown in Fig. 18 and the agreement between the observed and calculated intensities improved significantly. The consequence of this disorder is that the pyramids surrounding the Pb cations become distorted and these cations result in having three nearest neighbors (one O1 and two O2) and two O2 further away. The three nearest O atoms form a triangle with the 'lone pair' of electrons of the Pb^{2+} cations pointing along the perpendicular to the triangle. The orthorhombicity of the structure occurs because the disorder is different along x and y.

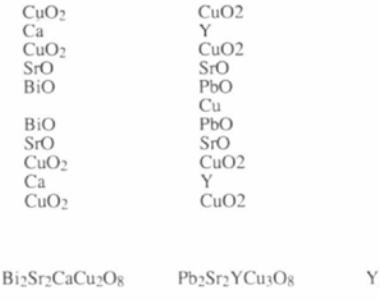

Fig. 16. (AO) and (BO_2) sequences in $Pb_2Sr_2YCu_3O_8$ (center), $YBa_2Cu_3O_6$ (right) and $Bi_2Sr_2CaCu_2O_8$ (left).

Hewat, Capponi, Cava, Chaillout, Marezio & Tholence (1989) and Zandbergen, Kadowski, Menken, Menovsky, Van Tendeloo & Amelinckx (1989) showed that electron diffraction patterns perpendicular to [001] for $Pb_2Sr_2YCu_3O_8$ and $Pb_2Ba_2YCu_3O_8$ each contained very weak well defined $hk0$ diffraction spots with $h+k$ odd, which violates the C centering. This indicated that the small displacements of the O atoms in the PbO layers are ordered. Subsequently, by taking into account the extra reflections, Fu, Zandbergen, Haije & De Jongh (1989) determined from powder neutron diffraction data that the most probable space group for $Pb_2Ba_2YCu_3O_8$ is $P22_12$. This corresponds to choosing in an ordered way one of the four (xyz) positions around a given 00z position. A recent structural determination based on single-crystal neutron data of superconducting $Pb_2Sr_2Y_{0.73}Ca_{0.27}Cu_3O_8$ (Chaillout, Chmaissem, Capponi, McIntyre & Marezio 1991) strongly indicated that the correct space group, at least for this compound, is *Pman*.

As stated above, one of the common features between $Pb_2Sr_2YCu_3O_8$ and $YBa_2Cu_3O_6$ is the presence of the oxygen-depleted (Cu) layers. As in the case of $YBa_2Cu_3O_6$, $Pb_2Sr_2YCu_3O_8$ can take up oxygen as well. No trace of superconductivity has been

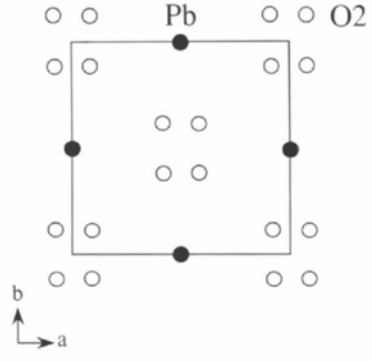

Fig. 18. Schematic representation of the PbO plane. The O2 atoms are disordered over the positions indicated by the open circles. For clarity the difference between x and y of the oxygen atoms has been exaggerated.

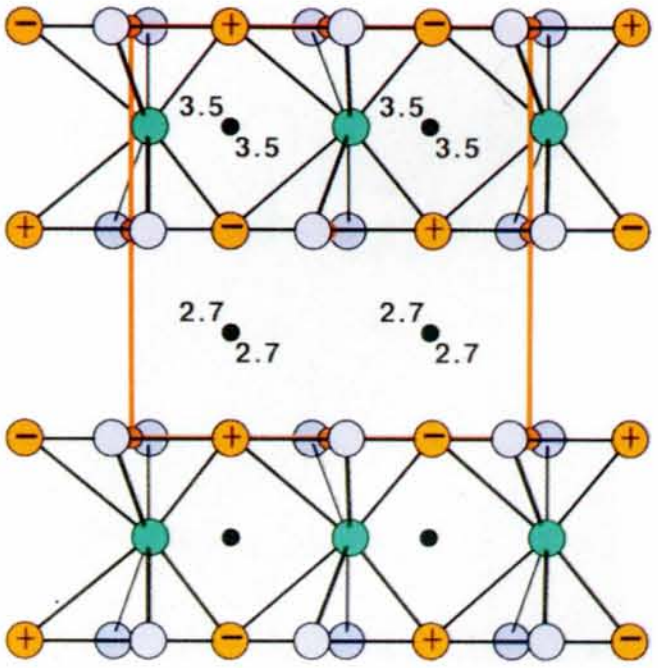

(*a*)

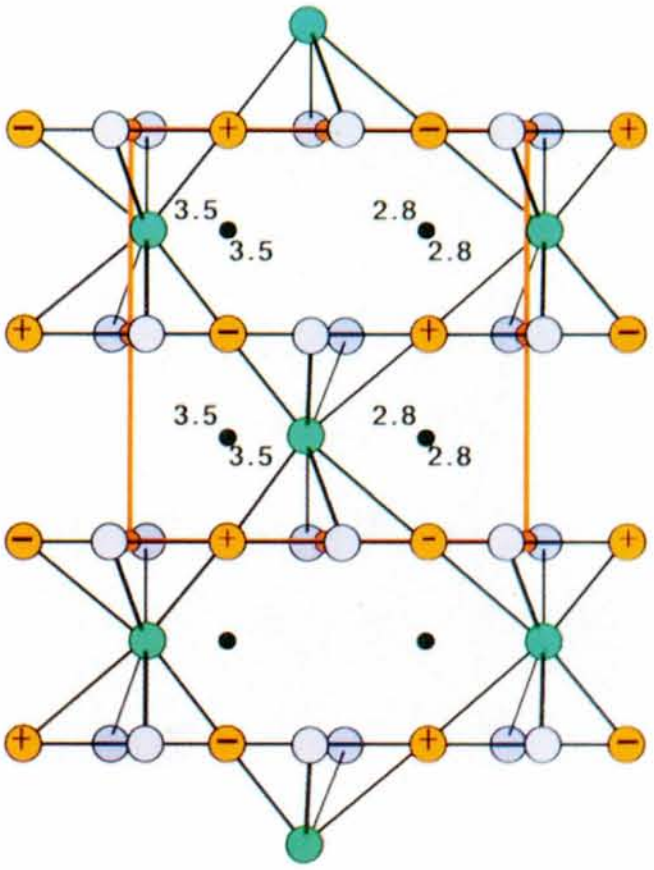

(*b*)

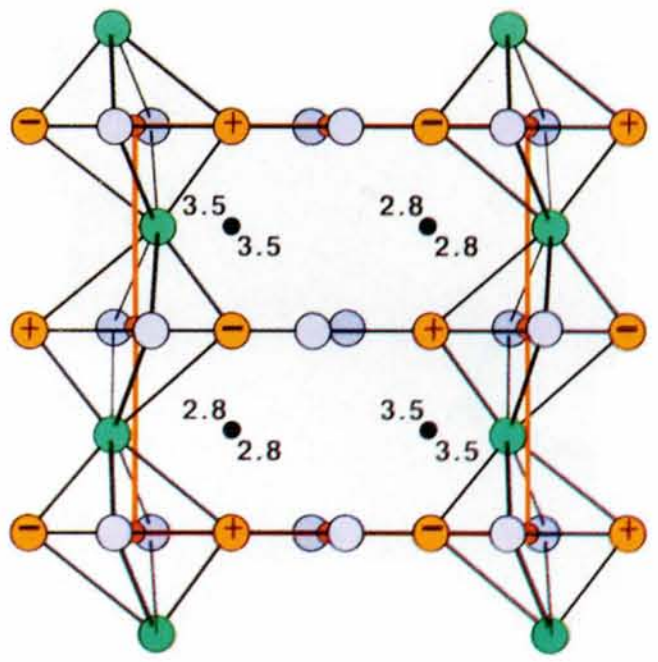

(*c*)

Fig. 26. (*a*), (*b*), (*c*) The same as Fig. 25, the superstructures correspond to $n_{O4} = 1{\cdot}00$ and $n_{O5} = 0{\cdot}5$. The $2a \times 2b$ supercells are outlined in orange.

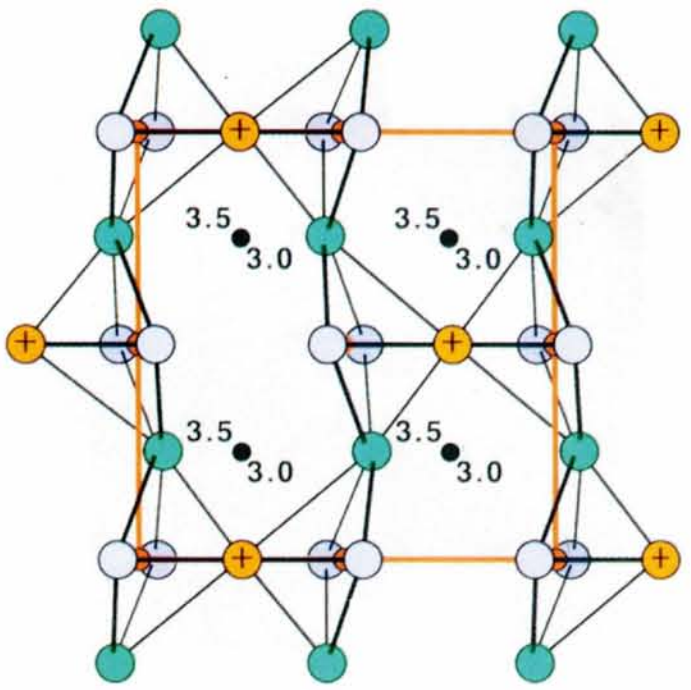

(*a*)

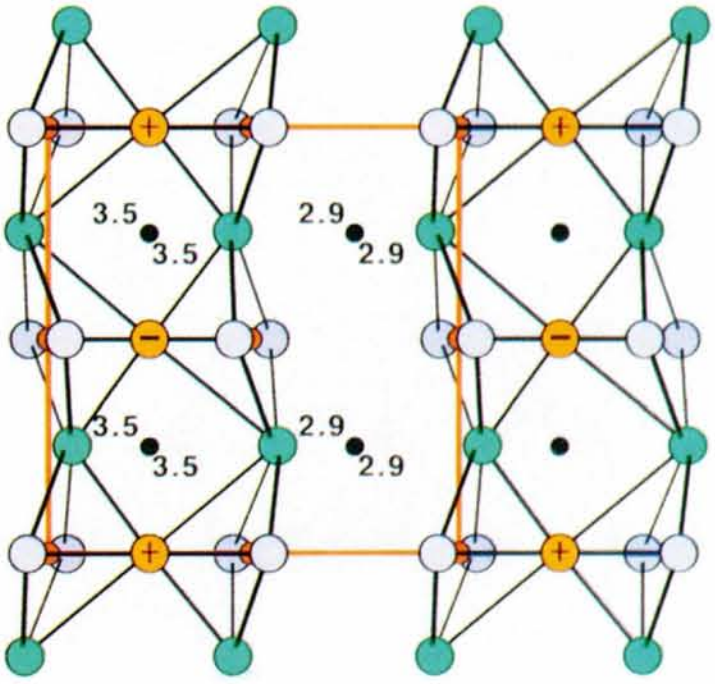

(*b*)

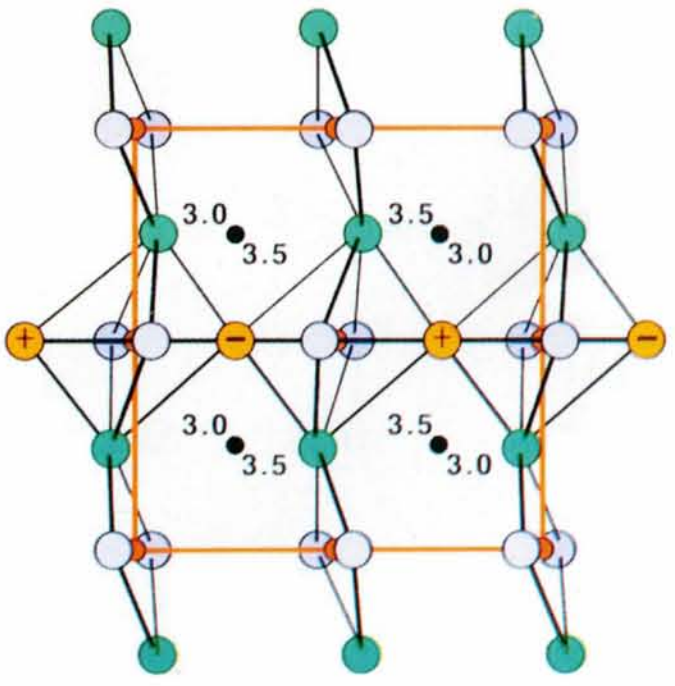

(*c*)

Fig. 27. (*a*), (*b*), (*c*) The same as Fig. 25, the superstructures correspond to $n_{O4} = 0{\cdot}5$ and $n_{O5} = 1{\cdot}00$. The $2a \times 2b$ supercells are outlined in orange.

detected so far in any oxidized sample of the latter compound whereas semiconducting $YBa_2Cu_3O_6$ can be fully oxidized to the 90 K superconductor $YBa_2Cu_3O_7$.

Fig. 19 shows the weight gain as a function of time when $Pb_2Sr_2YCu_3O_8$ is heat treated at 720 K in O_2 atmosphere. After about twenty hours the oxygen stoichiometry corresponds to $O_{9\cdot9}$ indicating that about two O atoms per molecule are incorporated in $Pb_2Sr_2YCu_3O_8$ as compared to one O atom per molecule in $YBa_2Cu_3O_6$. Conversely, if the final product $Pb_2Sr_2YCu_3O_{9\cdot9}$ is heat treated at 770 K in N_2 atmosphere it loses oxygen and goes back to O_8 stoichiometry as shown by the reduction curve in Fig. 19 (Capponi *et al.*, 1989).

As for $Pb_2Sr_2YCu_3O_8$, the oxidized samples are orthorhombic. However, the crystallographic axes are along those of the perovskite cell and the space group is *Pmmm*. The degree of orthorhombicity of the oxidized samples depends on the heat-treatment temperature and the cooling rate. Table 3 gives the lattice parameters for three typical samples. The first sample, corresponding to $\delta = 0$, is orthorhombic with a unit cell $2^{1/2}a_p \times 2^{1/2}a_p$ and $c = 15{\cdot}717$ Å; the second, oxidized to $\delta = 1{\cdot}40$ at 720 K in O_2, has an orthorhombic unit cell $a_p \times a_p$ and $c = 15{\cdot}845$ Å. The third sample, which was oxidized at 770 K in O_2, corresponding to $\delta = 1{\cdot}37$, has a tetragonal cell (a_p and $c = 15{\cdot}822$ Å). This sample must be orthorhombic but is found to be tetragonal because the orthorhombic crystallites are twinned along the (110) plane of the simple perovskite cell and the dimensions of the twin domains are smaller than the diffraction correlation length. Thus the powder diffraction technique cannot detect the difference between the a and b axes.

Fig. 20 shows the variation as a function of δ of the c parameter for $Pb_2Sr_2YCu_3O_{8+\delta}$ samples. It can be seen that for the interval $0{\cdot}4 < \delta < 1{\cdot}0$ the sample contains two phases, one corresponding to $\delta = 0$ and one to $\delta > 1$. This can be interpreted as an indication that when a sample with O_8 stoichiometry begins to incorporate oxygen domains are formed, each corresponding to one of two oxygen stoichiometries. Since the powder X-ray diffraction patterns indicate the presence of two phases the domains must be larger than the X-ray diffraction correlation length. For a certain value of δ greater than 1 all the Cu layers have the composition CuO_δ, the sample becomes single phased and the c parameter increases with increasing δ. It is worth mentioning that the oxidation process of $YBa_2Cu_3O_6$ produces chain fragments and is gradual, while that of $Pb_2Sr_2YCu_3O_{8+\delta}$ for δ included between 0 and a given value δ_x greater than 1 seems to produce blocks in which the stoichiometry is $O_{8+\delta_x}$.

Table 3. *Lattice parameters* (Å) *of* $Pb_2Sr_2YCu_3O_{8+\delta}$ (*from Capponi et al.*, 1989)

$\delta = 0$ as prepared	$\delta = 1{\cdot}40$; 720 K in O_2	$\delta = 1{\cdot}37$; 770 K in O_2
$a \simeq b = 2^{1/2}a_p$	$a \simeq b \simeq a_p$	$a \simeq b \simeq a_p$
$a = 5{\cdot}389\ (3)$	$a = 3{\cdot}838\ (2)$	$a = 3{\cdot}848\ (3)$
$b = 5{\cdot}428\ (3)$	$b = 3{\cdot}870\ (2)$	$b = 3{\cdot}848\ (3)$
$c = 15{\cdot}717\ (8)$	$c = 15{\cdot}845\ (8)$	$c = 15{\cdot}822\ (8)$

Fig. 21(a) shows the electron diffraction pattern perpendicular to [001] for $Pb_2Sr_2YCu_3O_8$. Note the presence of the $hk0$ spots for which $h + k = 2n + 1$ breaking the C centering. Spots away from the origin of the reciprocal lattice show splitting due to twinning by the (110) plane which is the (100) plane of the simple perovskite cell. Fig. 21(b) shows the corresponding pattern for a sample which has been oxidized to $\delta = 1{\cdot}4$. It can be seen that the oxidation is accompanied by a rotation of 45° of the basal crystallographic axes. The crystals are still twinned by the (110) plane. Because of the rotation of the crystallographic axes the twin individuals have also been rotated 45°. A superstructure for which both a and b axes have been doubled is visible in Fig. 21(b). Fig. 22(a) shows the electron diffraction pattern along [001] for another $Pb_2Sr_2YCu_3O_{9\cdot4}$ sample. A superstructure in which one of the basal axes has been multiplied by four and the other by two is seen.

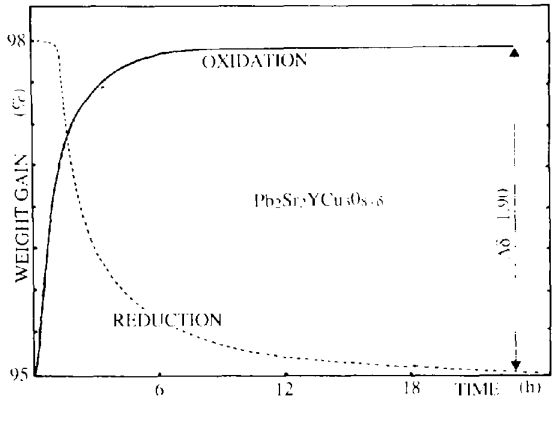

Fig. 19. Weight gain (solid line) and loss (dotted line) when $Pb_2Sr_2YCu_3O_8$ is heat treated at 720 K in O_2 and 770 K in N_2, respectively.

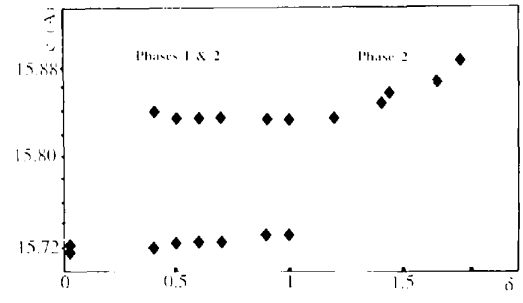

Fig. 20. Variation as a function of δ of the c parameter of $Pb_2Sr_2YCu_3O_{8+\delta}$.

Fig. 22(*b*) shows an electron diffraction pattern along one of the basal axes for the same oxidized sample. One can see the fourfold superstructure. All oxidized samples examined by electron diffraction showed some inhomogeneity with respect to the superstructure present. While the basic superstructure with unit cell $4a \times 2b \times c$ is seen in almost all samples, other superstructures are also seen. Moreover, additional weak spots indicating $8a$ and $2c$ periodicity are seen in some patterns.

It is evident that the extra O atoms which are incorporated in a $Pb_2Sr_2YCu_3O_8$ sample are located in the (Cu) layers sandwiched between two (PbO) ones. Since direct evidence for a given model is always more reassuring than speculation – even a sound one – we have carried out a structural determination of an oxidized sample by powder neutron diffraction (Marezio, Santoro, Capponi, Hewat, Cava & Beech, 1990). The oxygen content as determined by thermogravimetry was $O_{9\cdot41}$. The excess oxygen was found to be located on the (Cu1) layers at the position $(0, \frac{1}{2}, 0\cdot463) \equiv$ O4 with an occupancy factor equal to $0\cdot171(7)$ and at the position $(\frac{1}{2}, 0\cdot206, \frac{1}{2}) \equiv$ O5 with an occupancy factor equal to $0\cdot158(7)$. There are two O4 and two O5 positions per unit cell – one at $(0, \frac{1}{2}, z)$ and the other at $(0, \frac{1}{2}, \bar{z})$ for O4 and one at $(\frac{1}{2}, y, \frac{1}{2})$ and the other at $(\frac{1}{2}, \bar{y}, \frac{1}{2})$ for O5. Of the two positions for each set, only one can be occupied, otherwise unreasonable O–O distances are obtained.

The O2 atoms exhibit large thermal parameters in the *xy* plane which have been interpreted as due to

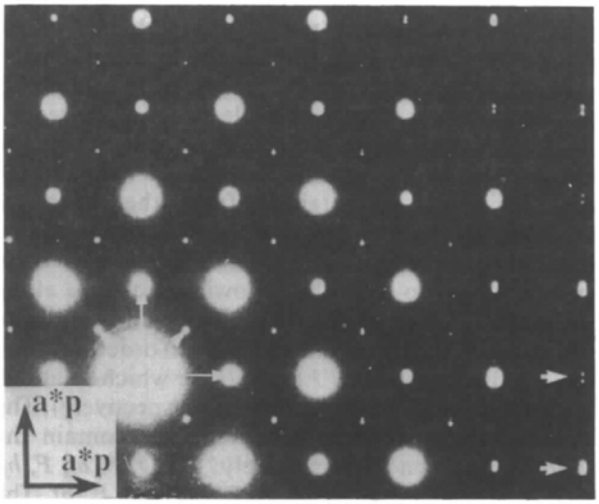

(*a*)

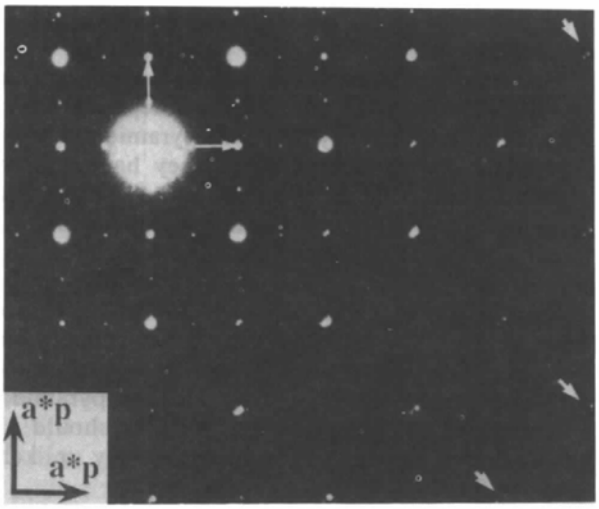

(*b*)

Fig. 21. (*a*) Electron diffraction pattern perpendicular to [001] for $Pb_2Sr_2YCu_3O_8$. (*b*) Electron diffraction pattern perpendicular to [001] for $Pb_2Sr_2YCu_3O_{9\cdot4}$.

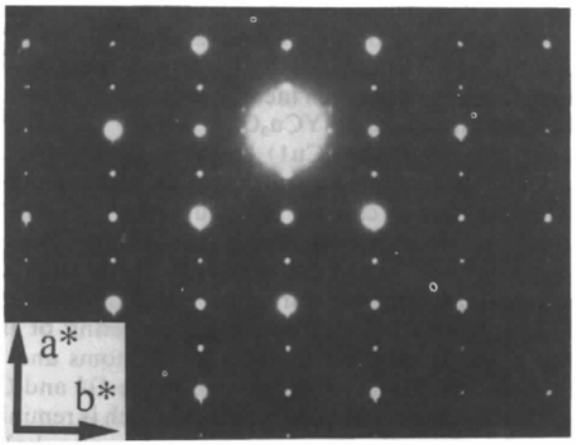

(*a*)

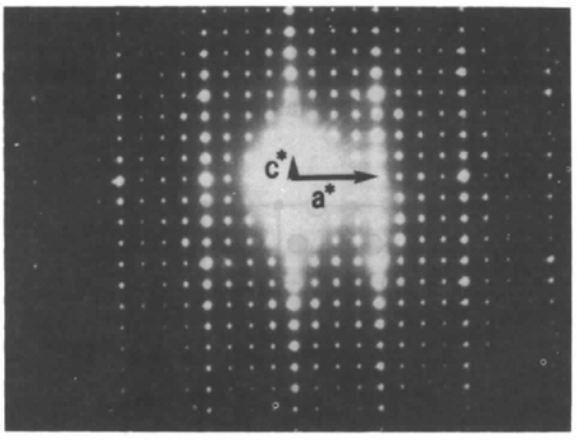

(*b*)

Fig. 22. (*a*) Electron diffraction pattern perpendicular to [001] for a sample of $Pb_2Sr_2YCu_3O_{9\cdot4}$ different from that of Fig. 21(*b*). (*b*) Electron diffraction pattern perpendicular to [010] for the same sample as that of (*a*).

disorder confined in the xy plane. Because of this high degree of disorder, in the refinements the O2 atom at $00z$ was put at the general position (xyz). However, convergence was attained only when it was put at the more symmetrical position ($0yz$). The thermal parameters, after the displacements had been taken into account, became more reasonable except along the x axis. This strongly indicates that the O2 atoms are also disordered along the x axis. But this disorder is either dynamic or static. In the latter case the correlation length must be shorter than that of the X-ray diffraction. It should be noted that the O1 atoms, belonging to the (SrO) layers, have a large thermal parameter along the y direction, but in the refinement, as in the case of O2 along the x axis, this atom could not be not displaced from the $\frac{1}{2}$ position along the y axis. It should be noted also that the oxygen incorporation induces the disorder only in the (PbO)(Cu)(PbO) blocks and in the oxygen of the (SrO) layers, *i.e.* oxygen which is bonded to the Pb cations. The $(CuO_2)(Y)(CuO_2)$ blocks seem to be unaffected by the oxygen incorporation. Fig. 23 shows the structure of $Pb_2Sr_2YCu_3O_{9\cdot5}$.

Fig. 24 shows the (Cu1) layers in which the Cu cations form an almost square lattice at $z=\frac{1}{2}$. After oxidation, in our case up to about $O_{9\cdot5}$, the extra O atoms are incorporated on this layer at the O4 sites $(0, \frac{1}{2}, 0{\cdot}46)$ and at the O5 sites $(\frac{1}{2}, 0{\cdot}21, \frac{1}{2})$. One can infer that the superstructures observed in the electron diffraction patterns are due to the ordering of the displacements of the O2, O4 and O5 atoms and to the ordering of the vacancies among the O4 and O5 sites. One simple way to order them, which is reminiscent of the $YBa_2Cu_3O_{6+x}$ system, is by forming chains parallel to the b axis. The displacements of the O2 and O4 atoms obtained independently during the refinement are consistent with each other as these atoms form a nearly perfect square. In this structure the Cu1 and Pb cations increase their coordination. Although in space group *Pmmm* all Cu1 and Pb sites are, respectively, crystallographically equivalent, more than one Cu1 and Pb sites are generated in the superstructures.

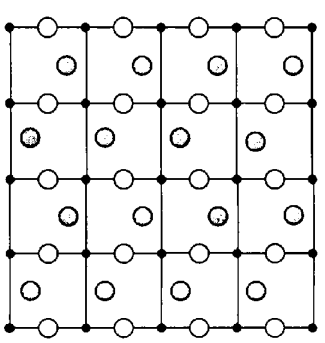

Fig. 24. The (CuO_x) layer. The black dots represent the Cu1 cations and the larger open and hatched circles the O4 and O5 atoms, respectively. The two oxygen sites are partially occupied.

The oxidation/reduction potentials of the Pb^{4+}/Pb^{2+} and the Cu^{3+}/Cu^{2+} systems indicate that, after the Cu^{+} cations of the (Cu) layers have been oxidized to Cu^{2+}, the oxidation of the Pb^{2+} cations to Pb^{4+} should take place prior to that of the Cu^{2+} cations to Cu^{3+} (or to Cu^{2+} and one electron hole). If one takes into account the fact that the oxidation of $Pb_2Sr_2YCu_3O_8$ does not induce superconductivity, one can infer that the extra positive charges, after the oxidation of Cu^{+} to Cu^{2+} has taken place, oxidize 50% of the Pb^{2+} to Pb^{4+} and that these two cations are ordered on the two Pb sites mentioned above. The extra positive charges would never reach the CuO_2 conduction planes, but would be trapped in the blocks which one would expect to act as an electron reservoir. Thus, the charge localization prevents the compound from becoming superconducting.

Fig. 25 shows simple possible superstructures for $Pb_2Sr_2YCu_3O_{9\cdot5}$, with a $4a\times2b\times c$ cell, when the extra O atoms are equally distributed over the O4 and O5 sites as obtained from the structural refinement. The full O4 and O5 sites form chains parallel to the b axis. The O4 chains are ordered in such a way as to form the following sequence along the a axis: *f, f, hf, hf, f, f* (in which *f* and *hf* indicate full and half-full chains). The O5 chain ordering along the a axis is, instead, *FFFEFFF* (in which *F* and *E* indicate full and empty O5 chains, respectively). The superstructures of Figs. 25(a) and (c) contain the following sequences respectively: *f, E, f, F, hf, F, hf, F, f, E, f* and *hf, E, hf, F, f, F, f, F, hf, E, hf*. The superstructures shown in Figs. 25(b) and (d) are obtained by interchanging the previous O4 and O5 orderings. The four superstructures correspond to a unit cell $4a\times2b\times c$ as indicated in the electron diffraction patterns.

The superstructures in Figs. 25(a) and (c) contain two and three crystallographically independent Cu1 sites, respectively. They are both pyramidally coordinated in the former, whereas they have square, pyramidal and octahedral coordination in the latter. The situation is more complicated in the superstructures shown in Figs. 25(b) and (d) where the Cu1 sites split into three and four crystallographically independent sites with different multiplicity. For example, the Cu1 cations have two different coordinations in Fig. 25(b) (tetrahedral and octahedral) while they have four in Fig. 25(d) (stick, square, pyramidal and octahedral). Since the Cu1 cations should all have valency 2+ this fourth model is very unlikely to occur for $\delta>1{\cdot}5$.

The coordination of the Pb cations also increases on going from $Pb_2Sr_2YCu_3O_8$ to $Pb_2Sr_2YCu_3O_{9\cdot5}$. All Pb sites are crystallographically equivalent in the former, they split into four or more inequivalent sites with different multiplicity in the latter and the Pb^{2+}

and Pb^{4+} cations become ordered. In Fig. 25 as well as in Figs. 26 and 27 the Pb cations are indicated by the valency calculated by the bond-length–bond-strength relationship and the constants given for Pb–O bonds by Brown & Altermatt (1985). The calculated values are far from being close to 2+ and 4+ in the 50/50 ratio as one would expect for $Pb_2Sr_2YCu_3O_{9\cdot5}$. The ordered sequences along the *a* axis of full, half-full and empty chains may be broken by some interchange, which might explain why the calculated Pb valences are 2·7, 2·8, 3·0 and 3·5 v.u. In addition, the large temperature factor of O1 indicates possible displacement of these atoms. The displacement of O1 away from the Pb cations would take place only when bonded to a Pb^{2+}, resulting in an increase of the Pb–O1 distance and consequent decrease of the corresponding bond strength and of the calculated valency of the Pb cation. When O1 is bonded to a Pb^{4+}, the displacement of O1 would occur towards the Pb cation, resulting in a decrease of the Pb–O1 distance and in an increase of the corresponding bond strength and of the calculated valency of the Pb cation. As can be seen from Figs. 25, 26 and 27, the ordering of these cations is different for each superstructure.

It seems unlikely that the Pb sites generated by the superstructures shown in Figs. 25(*b*) and (*d*) could accommodate Pb^{2+} and Pb^{4+} cations in a 50/50 ratio. In both cases there are ten sites for which the calculated valency is 3·4–3·5 v.u. and six with values ranging from 2·1 to 3·0. The most likely superstructures to occur in $Pb_2Sr_2YCu_3O_{9\cdot5}$ are those shown in Figs. 25(*a*) and (*c*). EXAFS measurements of these compounds should reveal the coordination of the Cu cations and shed some light as to which model is likely to occur for $\delta = 1\cdot5$.

As stated above, the structural refinement of a sample with $\delta = 1\cdot41$, determined by thermogravimetry, indicated that the extra O atoms are located on the O4 and O5 sites in about equal proportion (Marezio, Santoro, Capponi, Cava & Huang, 1991). But, if the location of the extra O atoms is definitely correct, their distribution is less certain. For this reason we present in Figs. 26(*a*), (*b*) and (*c*) and 27(*a*), (*b*) and (*c*) the possible superstructures obtained assuming full occupancy for the O4 sites and 50% occupancy for the O5 sites and *vice versa*, respectively. If the occupancy of the O4 and O5 sites has long-range order, the simplest superstructures would only have $2a \times 2b \times c$ unit cells as indicated in Figs. 26 and 27. The additional doubling of the *a* axis could be obtained by taking into account the O2 displacement along the *x* axis and those of O1 along the *y* axis, inferred from their large thermal factors. Because of the nearly crystallographic equivalence between O4 and O5, the arrangements of the two sets of superstructures shown in Figs. 26 and 27 are very similar. In two of them for each set all Cu1 cations have a pyramidal coordination while in the third superstructure half of the Cu1 cations have an octahedral coordination and the other half a square one.

These results strongly corroborate the conjecture that the extra positive charges are transferred from the (CuO_δ) layers to the (PbO) ones, do not reach the conduction layers (CuO_2) and that consequently the compound does not become a superconductor.

We have refined the structure of four $Pb_2Sr_2YCu_3O_{8+\delta}$ samples which had been oxidized according to the weight gain curve (Fig. 19) to different values of δ between 1 and 1·8. The oxygen stoichiometries as determined by powder neutron diffraction data ranged between 9·5 and 9·7. This seems to indicate that the compound with O_9 is very difficult to make. Since the oxidation takes place by layers it is possible that the oxidized layers reach the $O_{9\cdot5}$ stoichiometry directly and that the two phases, which are present after the oxidation, are $Pb_2Sr_2YCu_3O_8$ and one very close to $Pb_2Sr_2YCu_3O_{9\cdot5}$. This is consistent with the curve shown in Fig. 20. At $\delta = 1\cdot2$, the $Pb_2Sr_2YCu_3O_8$ phase was not detected because its percentage in the sample is too small. Furthermore, one would have to envisage rather complicated superstructures containing two sets of Pb sites with a ratio different from 1 : 1.

As shown by Cava, Batlogg, Krajewski, Farrow *et al.* (1988), $Pb_2Sr_2YCu_3O_8$ becomes superconducting at about 80 K when some of the trivalent Y cations are replaced by divalent Ca. This indicates that in this case the electron holes formed on the (Y, Ca) layer are transferred to the (CuO_2) conduction layers. Fig. 28 (curve *a*) represents the AC (alternating current) susceptibility *vs T* curve for a powder sample with the nominal $Pb_2Sr_2Y_{0\cdot5}Ca_{0\cdot5}Cu_3O_8$ composition. The onset of the superconductivity transition is at 78 K. However, the transition takes place over a large temperature interval and the superconducting volume can be estimated to be ~20%. This is probably due to an inhomogeneous distribution of the Ca cations over the Y sublattice. Fig. 29 represents the same type

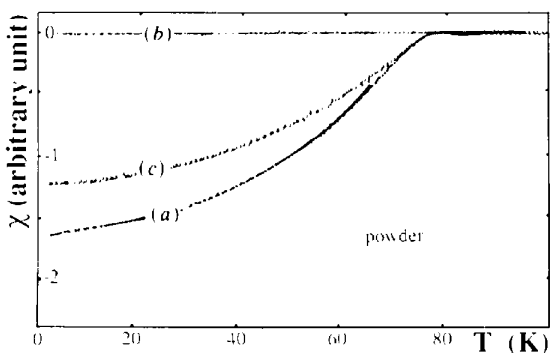

Fig. 28. AC susceptibility *vs T* for a $Pb_2Sr_2Y_{0\cdot5}Ca_{0\cdot5}Cu_3O_{8+\delta}$ sample: with $\delta = 0$ (curve *a*); after oxidation in O_2, $\delta = 1\cdot40$ (curve *b*); after reduction in N_2, $\delta = 0$ (curve *c*).

of measurements carried out on single-crystal samples grown in PbO flux and having approximately the same nominal $Pb_2Sr_2Y_{0.5}Cu_3O_8$ composition. The curves (*a*) and (*b*) correspond to two crystals from different batches. The different onsets, 55 and 80 K, respectively, may be due to different Ca concentrations in the two crystals resulting from small differences in the growth conditions (Capponi *et al.*, 1990). Note that for single-crystal samples the transition ΔT's are much narrower and the estimated superconducting volumes much larger (~100%) than those observed for powder samples.

It has been shown that T_c has a maximum around $x = 0{\cdot}5$ and decreases rapidly on each side. Fig. 30 shows how the AC susceptibility varies with x. For example, at $x = 0{\cdot}8$ only a small fraction of the sample, if any at all, becomes superconducting with an onset situated around 40 K.

When heat treated at 770 K in O_2 atmosphere, superconducting $Pb_2Sr_2Y_{0.5}Ca_{0.5}Cu_3O_8$ behaves similarly to $Pb_2Sr_2YCu_3O_8$. Fig. 28 (curve *b*) shows the AC susceptibility *vs* T curve for a $Pb_2Sr_2Y_{0.5}Ca_{0.5}Cu_3O_8$ sample after oxidation to $O_{9.4}$ stoichiometry.

As can be seen, the superconducting transition is suppressed. By heat treating this sample at 770 K in N_2 the superconducting properties are re-established (see Fig. 28, curve *c*) and the oxygen content is reduced to O_8. This is exactly the opposite to what happens for $YBa_2Cu_3O_6$, where oxygen incorporation leads to the appearance of superconductivity.

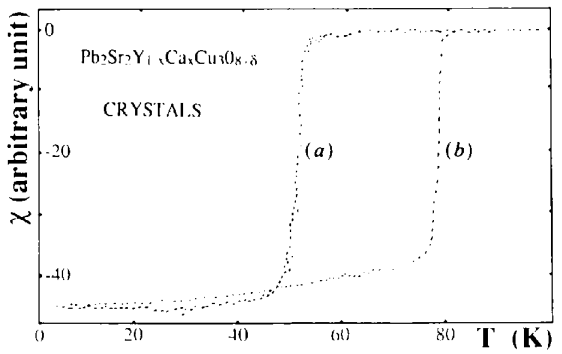

Fig. 29. AC susceptibility *vs* T for two single crystals with nominal composition $Pb_2Sr_2Y_{1-x}Ca_xCu_3O_8$ with $x = 0{\cdot}5$ and $\delta = 0$, from two different batches.

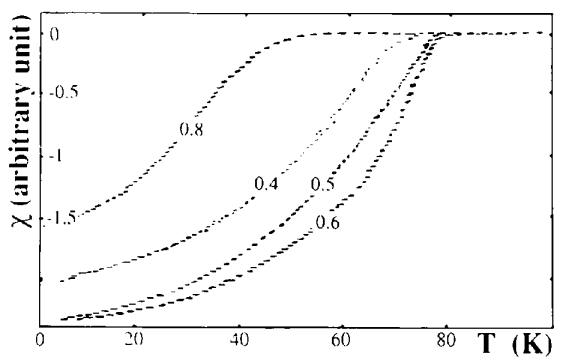

Fig. 30. AC susceptibility *vs* T for $Pb_2Sr_2Y_{1-x}Ca_xCu_3O_8$ samples with different x values.

The replacement of Y with Ca produces extra positive charges which are transferred to the CuO_2 conducting layers. Some of the Cu^{2+} cations are oxidized to Cu^{3+} (or to Cu^{2+} and one electron hole) and the compound is superconducting. Why are these charges not transferred to the (PbO)(Cu)(PbO) blocks as are those produced by oxygen incorporation? The (PbO)-(Cu)(PbO) blocks contain Cu^+ cations in stick coordination and Pb^{2+} cations in distorted pyramidal coordination. These cations cannot be oxidized without adding extra oxygen because the Cu^{2+} and Pb^{4+} cations would not be stable in two and five coordination, respectively. When $Pb_2Sr_2Y_{0.5}Ca_{0.5}Cu_3O_8$ begins to incorporate oxygen, the extra positive charges are located in the (PbO)-(Cu)(PbO) blocks just as in $Pb_2Sr_2YCu_3O_8$ and the oxidation of Cu^+ and Pb^{2+} occurs. The oxidation of the latter cations induces the displacement of the O1 atoms of the (SrO) layers towards the Pb^{4+} cations and away from the CuO_2 layers. The apical pyramidal Cu2–O1 distances increase, which is equivalent to a charge transfer from the pyramidal CuO_2 layers to the $(PbO)(CuO_\delta)(PbO)$ blocks where the charges become localized. This charge transfer and consequent localization are responsible for the suppression of the superconducting properties.

Concluding remarks

I have presented the results of superconductivity property measurements, electron diffraction studies and powder neutron diffraction structural determinations for the two systems $YBa_2Cu_3O_{6+x}$ and $Pb_2Sr_2Y_{1-x}Ca_xCu_3O_{8+\delta}$. For the former, oxygen incorporation leads to the appearance of the superconducting properties. Our results on the addition of oxygen to $YBa_2Cu_3O_6$ suggest that superconductivity at ~60 K appears when 0·05 positive charges per Cu cation are abruptly transferred at about $x = 0{\cdot}45$ from the linear Cu cations to the planar Cu cations. The increase of T_c from 60 to 90 K occurs when a gradual transfer of 0·03 positive charges per Cu cation occurs between $x = 0{\cdot}66$ and $x = 0{\cdot}84$ from the linear Cu cations to the planar Cu cations.

For non-superconducting $Pb_2Sr_2YCu_3O_8$ which is the counterpart of $YBa_2Cu_3O_6$ the incorporation of oxygen does not induce superconductivity. The oxygen addition to $Pb_2Sr_2YCu_3O_8$ induces the oxidation of the Cu^+ and Pb^{2+} cations to Cu^{2+} and Pb^{4+}, respectively. The extra positive charges never reach the CuO_2 conducting planes, but are localized in the $(PbO)(CuO_\delta)(PbO)$ blocks.

The oxygen incorporation in superconducting $Pb_2Sr_2Y_{0.5}Ca_{0.5}Cu_3O_8$ suppresses the superconducting properties. Just as in $Pb_2Sr_2YCu_3O_8$ the extra positive charges are located in the (PbO)(Cu)(PbO) blocks inducing the oxidation of Cu^+ and Pb^{2+} to Cu^{2+} and Pb^{4+}, respectively. In order to generate the appropriate coordination for Pb^{4+} the O1 atoms of the (SrO) layers are displaced and a charge transfer occurs from the $(CuO_2)(Y, Ca)(CuO_2)$ blocks to the $(PbO)(CuO_\delta)(PbO)$ ones.

In both systems, $YBa_2Cu_3O_{6+x}$ and $Pb_2SrY_{1-x}Ca_xCu_3O_{8+\delta}$, the oxygen incorporation induces a rearrangement of the O atoms already present in the structure. A crucial oxygen for both compounds is the apical oxygen of the CuO_5 pyramidal layers sandwiching the oxygen-depleted yttrium layers.

Besides presenting our latest results on the oxygen stoichiometry problem in two high-T_c superconductor series, I have tried to show that one can relate physical properties such as superconductivity to structural properties provided that the 'real' structure is determined. In order to get the 'real' structure or at least the closest model to it, one must use all diffraction techniques available, such as X-ray and neutron diffraction, electron microscopy and also X-ray absorption techniques.

This article could not have been written without the collaboration of my colleagues at the CNRS, Grenoble, P. Bordet, J. J. Capponi, C. Chaillout, O. Chmaissen, J. Chenavas, J. L. Hodeau, B. Souletie, P. Strobel and J. L. Tholence, of A. W. Hewat of the Institut Laue-Langevin, Grenoble, of E. A. Hewat of the CEN, Grenoble, of A. Santoro of NIST, Gaithersburg, MD, and of B. Batlogg and R. J. Cava of AT&T Bell Laboratories, Murray Hill, NJ.

References

ALARIO-FRANCO, M. A., CHAILLOUT, C., CAPPONI, J. J., CHENAVAS, J. & MAREZIO, M. (1987). *Mater. Res. Soc. Symp. Proc.* **99**, 41-47.

BEECH, F., MIRAGLIA, S., SANTORO, A. & ROTH, R. S. (1987). *Phys. Rev. B*, **35**, 8778-8781.

BENO, M. A., SODERHOLM, L., CAPONE, D. W. II, HINKS, D. G., JORGENSEN, J. D., SCHULLER, I. K., SEGRE, C. U., ZHANG, K. & GRACE, J. D. (1987). *Appl. Phys. Lett.* **51**, 57-59.

BEYERS, R., AHN, B. T., GORMAN, G., LEE, V. Y., PARKIN, S. S. P., RAMIREZ, M. L., ROCHE, K. P., VAZQUEZ, J. E., GÜR, T. M. & HUGGINS, R. A. (1989). *Nature (London)*, **340**, 619-621.

BORDET, P., CHAILLOUT, C., CAPPONI, J. J., CHENAVAS, J. & MAREZIO, M. (1987). *Nature (London)*, **327**, 687-689.

BROWN, I. D. (1989) *J. Solid State Chem.* **82**, 122-131.

BROWN, I. D. (1990). Proc. of the Int. Conf. on the Chemistry of Electronic Ceramic Materials, Jackson Hole, WY, USA, August 1990, pp. 471-481.

BROWN, I. D. & ALTERMATT, D. (1985) *Acta Cryst.* B**41**, 244-247.

CAPPONI, J. J., BORDET, P., CHAILLOUT, C., CHENAVAS, J., CHMAISSEN, O., HEWAT, E. A., HODEAU, J. L., KORCZAK, W. & MAREZIO, M. (1989). *Physica (Utrecht)*, C**162-164**, 153-154.

CAPPONI, J. J., CHAILLOUT, C., HEWAT, A. W., LEJAY, P., MAREZIO, M., NGUYEN, N., RAVEAU, B., SOUBEYROUX, J. L., THOLENCE, J. L. & TOURNIER, R. (1987). *Europhys. Lett.* **3**, 1301-1307.

CAPPONI, J. J., CHMAISSEN, O., FOURNIER, T., GORIUS, M. F., KORCZAK, S., MAREZIO, M. & THOLENCE, J. L. (1990). *J. Less Common Met.* **164 & 165**, 808-815.

CAVA, R. J. (1987). *Int. J. Mod. Phys.* **1**, 813-820.

CAVA, R. J., BATLOGG, B., VAN DOVER, R. B., KRAJEWSKI, J. J., WASZCZAK, J. V., FLEMING, R. M., PECK, W. F. JR, RUPP, L. W. JR, MARSH, P., JAMES, A. C. W. P. & SCHNEEMEYER, L. F. (1990). *Nature (London)*, **345**, 602-604.

CAVA, R. J., BATLOGG, B., KRAJEWSKI, J. J., FARROW, R. C., RUPP, L. W. JR, WHITE, A. E., SHORT, K. T., PECK, W. F. JR & KOMETANI, T. Y. (1988). *Nature (London)*, **332**, 814-816.

CAVA, R. J., BATLOGG, B., KRAJEWSKI, J. J., RUPP, L. W. JR, SCHNEEMEYER, L. F., SIEGRIST, T., VAN DOVER, R. B., MARSH, P., PECK, W. F. JR, GALLAGHER, P. K., GLARUM, S. H., MARSHALL, J. H., FARROW, R. C., WASZCZAK, J. V., HULL, R. & TREVOR, P. (1988). *Nature (London)*, **336**, 211-214.

CAVA, R. J., HEWAT, A. W., HEWAT, E. A., BATLOGG, B., MAREZIO, M., RABE, K. M., KRAJEWSKI, J. J., PECK, W. F. JR & RUPP, L. W. JR (1990). *Physica (Utrecht)*, C**165**, 419-433.

CAVA, R. J., MAREZIO, M., KRAJEWSKI, J. J., PECK, W. F. JR, SANTORO, A. & BEECH, F. (1989). *Physica (Utrecht)*, C**157**, 272-278.

CHAILLOUT, C., CHMAISSEM, O., CAPPONI, J. J., MCINTYRE, G. & MAREZIO, M. (1991). *Physica (Utrecht)*, C**175**, 293-300.

COX, D. E., MOODENBAUGH, A. R., HURST, J. J. & JONES, R. H. (1987). *J. Phys. Chem. Solids*, **49**, 47-52.

DAVID, W. I. F., HARRISON, W. T. A., GUNN, J. M. F., MOZE, O., SOPER, A. K., DAY, P., JORGENSEN, J. D., HINKS, D. G., BENO, M. A., SODERHOLM, L., CAPONE, D. W. II, SCHULLER, I. K., SEGRE, C. U., ZHANG, K. & GRACE, J. D. (1987). *Nature (London)*, **327**, 310-312.

FRANÇOIS, M., WALKER, E., JORDA, J. L., YVON, K. & FISCHER, P. (1987). *Solid State Commun.* **63**, 1149-1153.

FU, W. T., ZANDBERGEN, H. W., HAIJE, W. G. & DE JONGH, L. J. (1989). *Physica (Utrecht)*, C**159**, 210-214.

GREEDAN, J. E., O'REILLY, A. H. & STAGER, C. V. (1987). *Phys. Rev. B*, **35**, 8770-8773.

HEWAT, E. A., CAPPONI, J. J., CAVA, R. J., CHAILLOUT, C., MAREZIO, M. & THOLENCE, J. L. (1989). *Physica (Utrecht)*, C**157**, 509-514.

HINKS, D. G., DRABOWSKI, B., JORGENSEN, J. D., MITCHELL, A. W., RICHARDS, D. R., PEI, S. & SHI, D. (1988). *Nature (London)*, **333**, 836-838.

IZUMI, F., ASANO, H., ISHIGAKI, T., TAKAYAMA-MUROMACHI, E., UCHIDA, Y., WANATABE, N. & NISHIKAWA, T. (1987). *Jpn. J. Appl. Phys.* **26**, L649-651.

JORGENSEN, J. D., VEAL, B. W., PAULIKAS, A. P., NOWICKI, L. J., CRABTREE, G. W., CLAUS, H. & KWOK, W. K. (1990). *Phys. Rev. B*, **41**, 1863-1877.

MAREZIO, M., SANTORO, A., CAPPONI, J. J., CAVA, R. J. & HUANG, C. (1991). In preparation.

MAREZIO, M., SANTORO, A., CAPPONI, J. J., HEWAT, E. A., CAVA, R. J. & BEECH, F. (1990). *Physica (Utrecht)*, C**169**, 401-412.

MATTHEISS, L. F., GYORGY, E. M. & JOHNSON, D. W. JR (1988). *Phys. Rev. B*, **37**, 3745-3746.

SANTORO, A., BEECH, F., MAREZIO, M. & CAVA, R. J. (1988). *Physica (Utrecht)*, **156**, 693-700.

SANTORO, A., MIRAGLIA, S., BEECH, F., SUNSHINE, S. A., MURPHY, D. W., SCHNEEMEYER, L. F. & WASZCZAK, J. V. (1987). *Mater. Res. Bull.* **22**, 1007-1013.

SCHNEEMEYER, L. F., THOMAS, J. K., SIEGRIST, T., BATLOGG, B., RUPP, L. W. JR, OPILA, R. L., CAVA, R. J. & MURPHY, D. W. (1988). *Nature (London)*, **335**, 421-423.

SIEGRIST, T., SUNSHINE, S. A., MURPHY, D. W., CAVA, R. J. & ZAHURAK, S. M. (1987). *Phys. Rev. B*, **35**, 7137-7139.

STROBEL, P., CAPPONI, J. J., CHAILLOUT, C., MAREZIO, M. & THOLENCE, J. L. (1987). *Nature (London)*, **327**, 306-308.

SUBRAMANIAN, M. A., GOPALAKRISHNAM, J., TORARDI, C. C., GAI, P. L., BOYES, E. D., ASKEW, T. R., FLIPPEN, R. B., FARNETH, W. E. & SLEIGHT, A. W. (1989). *Physica (Utrecht)*, C**157**, 124-130.

TRANQUADA, J. M., COX, D. E., KANMANN, W., MOUDDEN, H., SHIRANE, G., SUENAGA, M., ZOLLIGER, P., VAKNIN, P., SINHA, S. K., ALVAREZ, M. S., JACOBSON, A. J. & JOHNSON, D. C. (1987). *Phys. Rev. Lett.* **60**, 156-159.

WU, M. K., ASHBURN, J. R., TORNG, C. J., HOR, P. H., MENG, R. L., GAO, L., HUANG, Z. J., WANG, Y. Z. & CHU, C. W. (1987). *Phys. Rev. Lett.* **58**, 908-910.

ZANDBERGEN, H. W., KADOWAKI, K., MENKEN, M. J. V., MENOVSKY, A. A., VAN TENDELOO, G. & AMELINCKX, S. (1989). *Physica (Utrecht)*, **158**, 155-172.